# Dark Energy with Galaxy Clustering

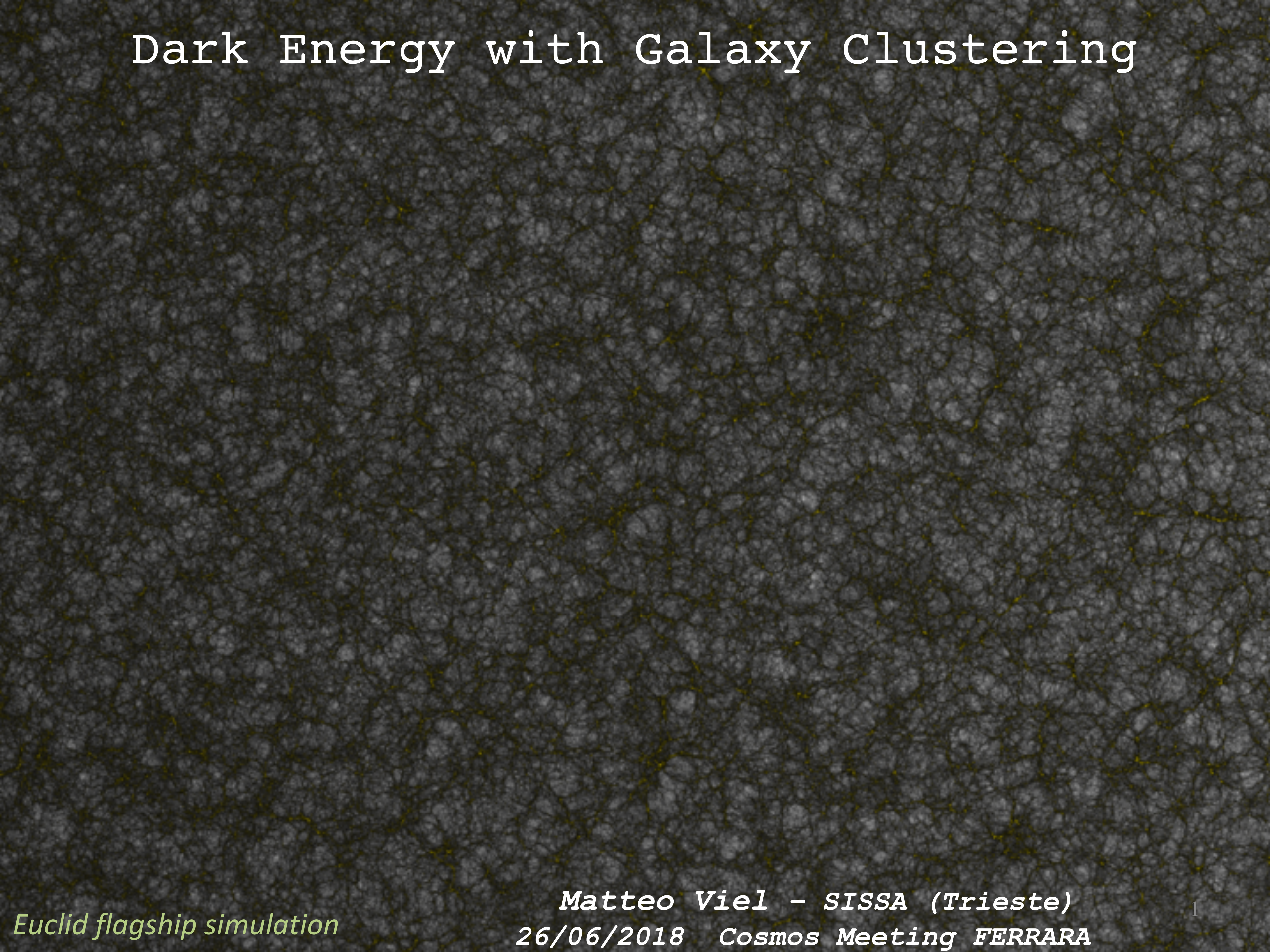

Euclid flagship simulation

***Matteo Viel – SISSA (Trieste)***

***26/06/2018 Cosmos Meeting FERRARA***

# Dark Energy after Planck - I

Planck Paper XIV "Dark Energy and Modified Gravity" (2016)

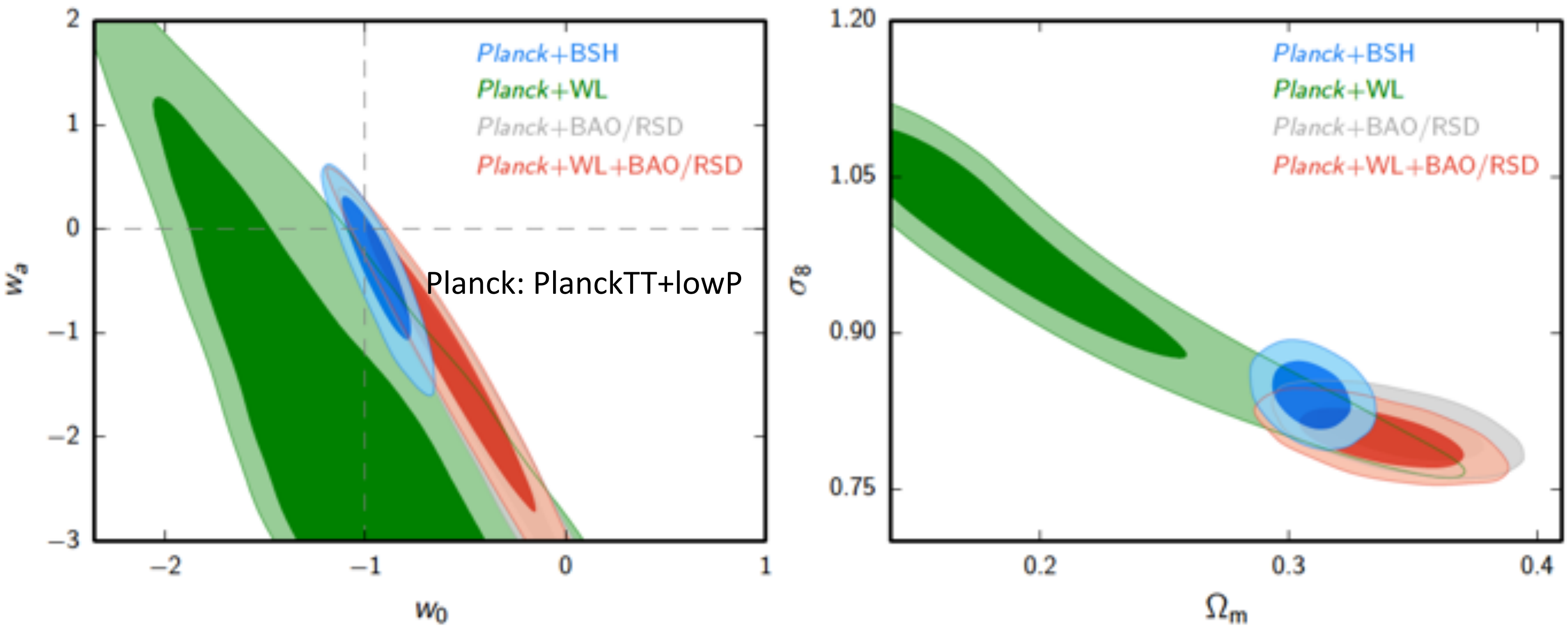


Planck+BSH combination has a $\Delta\chi^2$=−0.8 w.r.t. base LCDM

WL is CFHTLens: prefers $w_0$−$w_a$ at 2$\sigma$ w.r.t. LCDM, wants higher $\sigma_8$ and (not shown) high value of $H_0$

Implications for the small scale crisis of LCDM

# Dark Energy after Planck - II

Planck Paper XIV

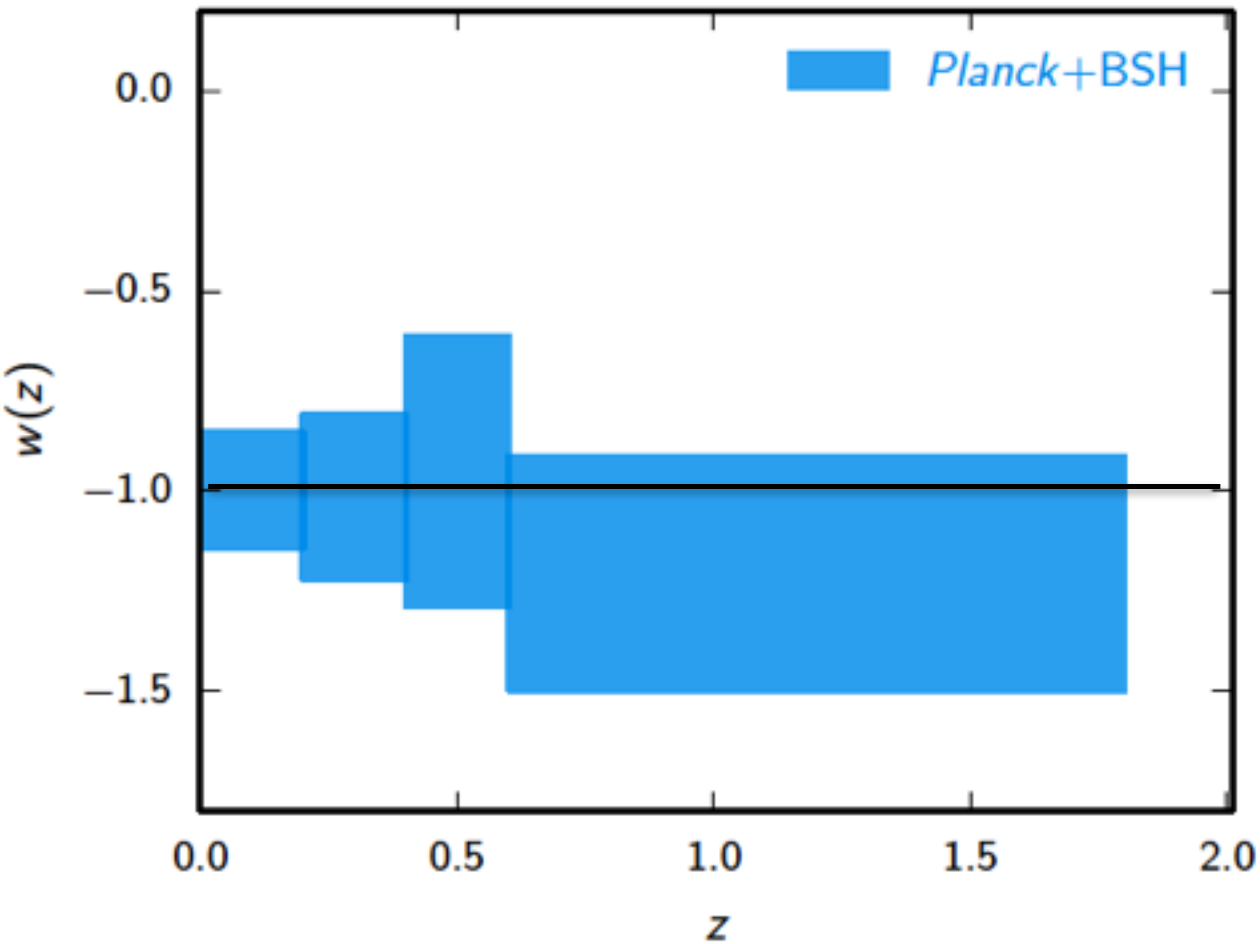


Principal Component Analysis reconstruction in 4 bins, increasing number of bins does lead to same conclusions.

$$w(z) = p_{i-1} + \Delta w \left( \tanh\left[ \frac{z - z_i}{s} \right] + 1 \right) \text{ for } z < z_i, \ \mathrm{i} \in \{1, 4\}$$

# Dark Energy after Planck - III

Planck Paper XIV

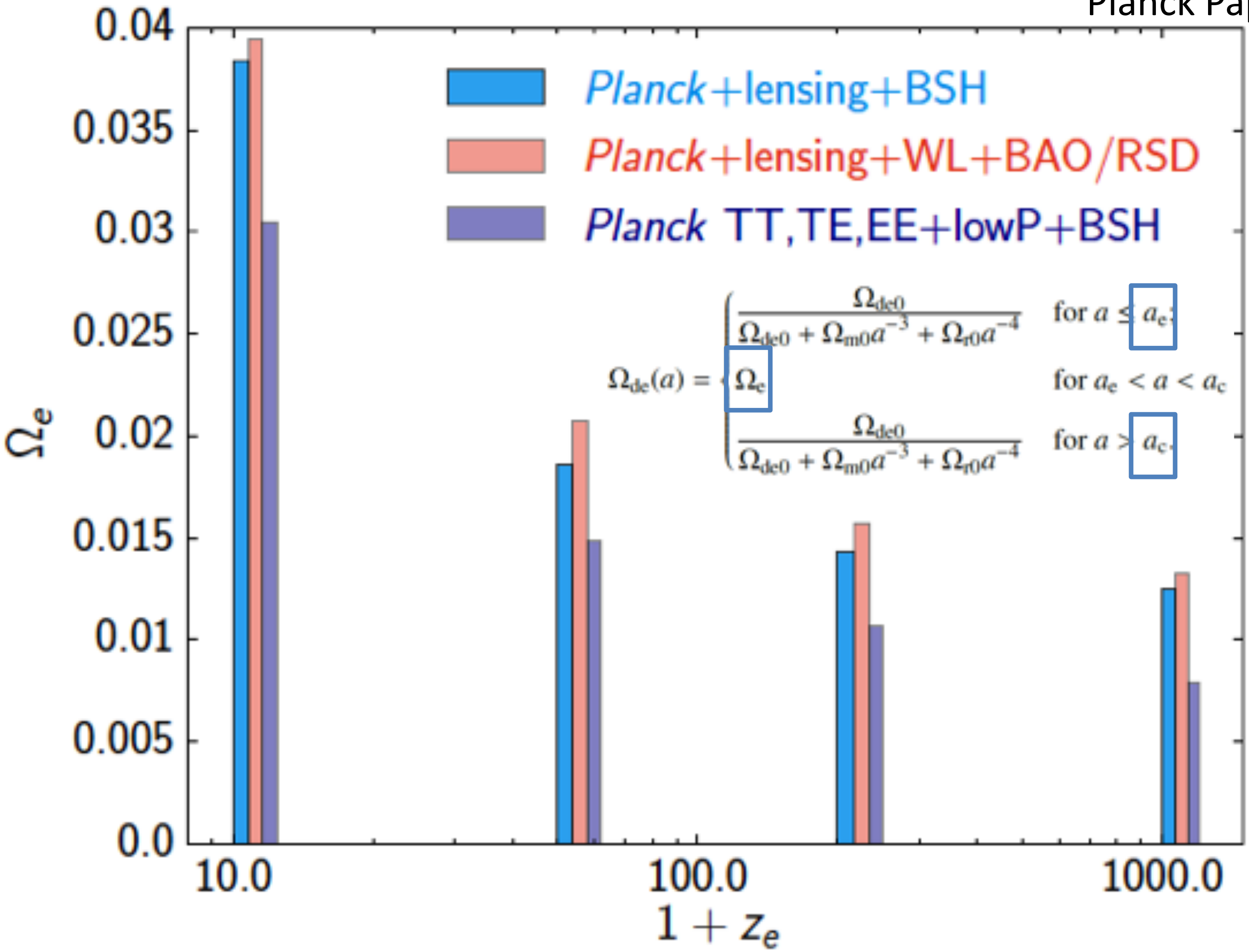


Note further that Planck is providing a measurement of the sound horizon at the drag epoch with an error of 0.2% …

# Dark Energy after Planck - IV

**Remarkable results from Planck experiment in constraining DE properties**

1) In ($w_0$-$w_a$), Planck TT+lowP+BSH is compatible with LCDM, as well as BAO/RSD. When adding WL to Planck TT+lowP, both WL and CMB prefer the ($w_0$-$w_a$) model with respect to LCDM at $\sim 2\sigma$ (with preference for high values of $H_0$, excluded when including BSH). CMB lensing does not change the numbers.

2) Tests on time varying w(z) are compatible with LCDM for all data sets tested.

3) EDE model with constant fraction till recent. Constraints are incredibly tight: previous constraints improved by a factor 3-4, $\Omega_e < 0.0036$ for PlanckTT,TE,EE+lowP+BSH. Polarization improves limits by a factor 2.

4) $\Omega_e(z)$ as a function of $z_e$, the redshift starting from which a fraction is present. $\Omega_e < 2\%$ (95% C.L.) even for $z_e$ as late as 50 (important results in the era of **structure formation** with implications for EDGES and other science). CMB lensing is important.

# The information in galaxy clustering

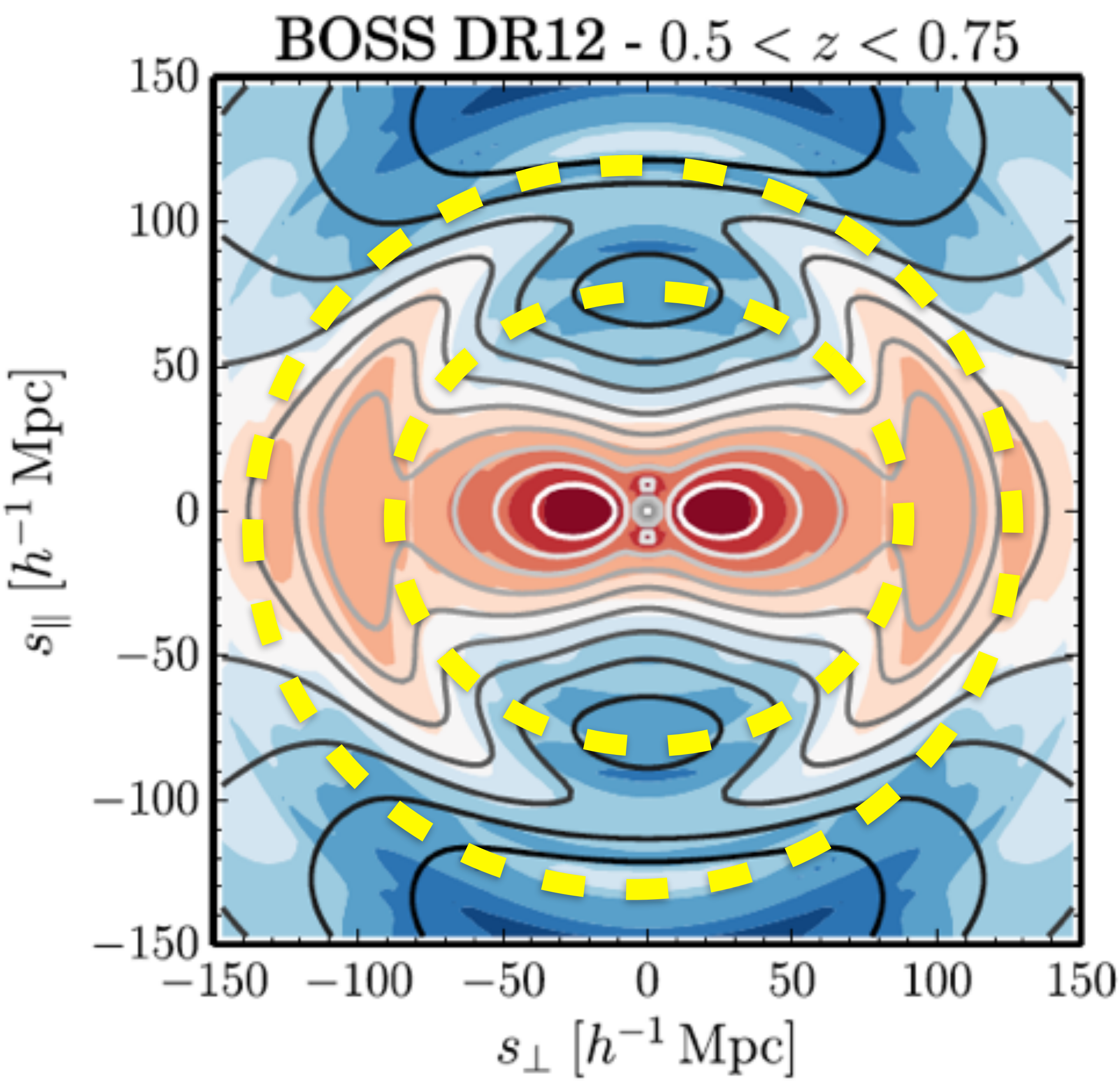


*What is galaxy clustering adding (if anything) to what we already know from the CMB results?*

# Galaxy Clustering - I: Theoretical Framework

Analysis of **anisotropic correlation function** focussed on the BAO signal

Two sources of anisotropies: Redshift Space Distortion (RSD)
Geometrical induced anisotropy (AP)

$$\xi(r,\mu) = \frac{DD(r,\mu) - 2DR(r,\mu) + RR(r,\mu)}{RR(r,\mu)}, \qquad \xi_\ell(r) = \frac{2\ell+1}{2}\int_{-1}^{+1} d\mu\, \xi(r,\mu)\, L_\ell(\mu)$$

**Non-linear modelling of correlation function**

$$P(k,\mu) = (1+\beta\mu^2)^2 F(k,\mu,\Sigma_s) P_{NL}(k,\mu).$$

$$F(k,\mu,\Sigma_s) = \frac{1}{(1+k^2\mu^2\Sigma_s^2)}$$

$$P_{dw}(k,\mu) = [P_{lin}(k) - P_{nw}(k)] \times \exp\left[-\frac{k^2\mu^2\Sigma_\parallel^2 + k^2(1-\mu^2)\Sigma_\perp^2}{2}\right] + P_{nw}$$

$$P_{l,t}(k) = \frac{2l+1}{2}\int_{-1}^{1} P_t(k,\mu) L_l(\mu) d\mu$$

$$\xi_{l,t}(r) = i^l \int \frac{k^3\, d\log(k)}{2\pi^2} P_{l,t}\, j_l(kr).$$

$$\xi_0(r) = B_0^2 \xi_{0,t}(r) + A_0(r),$$
$$\xi_2(r) = \xi_{2,t}(r) + A_2(r),$$

where

$$A_\ell(r) = \frac{a_{\ell,1}}{r^2} + \frac{a_{\ell,2}}{r} + a_{\ell,3};\ \ell = 0, 2, \perp, \parallel$$

# Galaxy Clustering - II: Theoretical Framework

$$\alpha = \alpha_\perp^{2/3}\alpha_{||}^{1/3},$$

$$1+\epsilon = \left(\frac{\alpha_{||}}{\alpha_\perp}\right)^{1/3}$$

$$\alpha_\perp = \frac{D_A(z) r_s^{\mathrm{fid}}}{D_A^{\mathrm{fid}} r_s}$$

$$\alpha_{||} = \frac{H^{\mathrm{fid}}(z) r_s^{\mathrm{fid}}}{H(z) r_s}$$

**α, ε** usually appear when referring to systematics/mocks while distances and $F_{AP}$ when quoting final cosmologically relevant numbers

$$D_V(z) = \left(D_M^2(z)\frac{cz}{H(z)}\right)^{1/3}$$

$$F_{\mathrm{AP}}(z) = D_M(z)H(z)/c.$$

# Galaxy clustering challenges - ca 2020

Measurement of galaxy clustering hampered by **systematics** and **statistical** errors.

Estimating the window function and selection function is not trivial.

Focus on:

1) optimization of codes to handle large number of objects
2) getting reliable mocks
3) quantifying systematic effects
4) covariance matrix estimation
5) improving **reconstruction techniques**

State-of-the-art provided by BOSS survey (e.g. Alam+18, Vargas-Magana+18)

1) Systematics are estimated and appear as weights in the selection function
2) Mock generation using several different methods - based on Perturbation theory or N-body simulations
3) Estimation of the 2D correlation function using Landy-Szalay estimator
4) Analysis focused on BAO peak and in second instance on sub-BAO **shape** info
5) Different pipelines tested with estimation of systematic errors introduced in each step
6) Main conclusions: unlike naively expected latest BOSS results **are dominated by statistical errors**

# Galaxy clustering: the data set

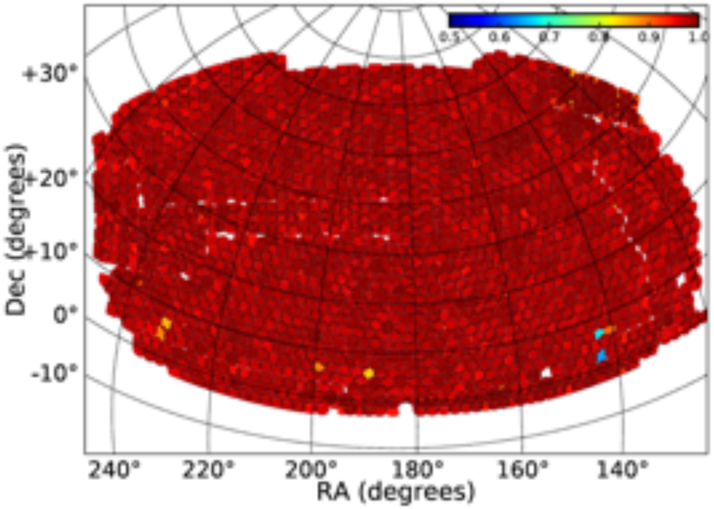


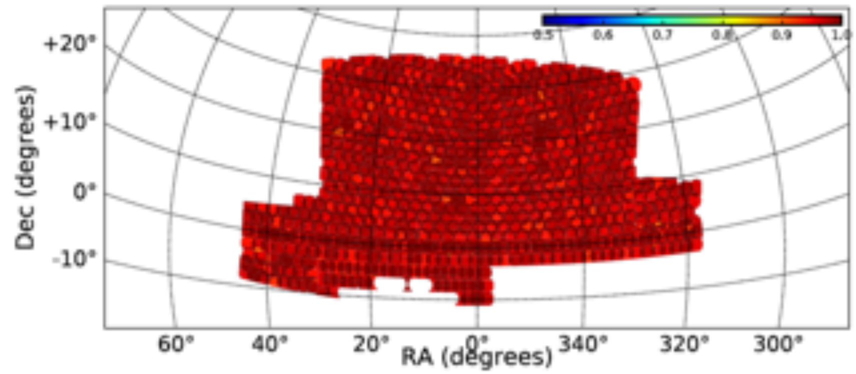


10,000 sq. deg. & 1.2 million galaxies in V=20 Gpc^3

medium-resolution spectra
(R ≈ 1500–2600) in the wavelength range
from 3600 to 10000 Å
through 2 arcsec fibres

LOWZ was designed
to target luminous red galaxies up to z ≈ 0.4, while CMASS
was designed to target massive galaxies
from 0.4 < z < 0.7

Seven data analyses performed with
different methodologies (tested on
mocks)

| | | $N_{gals}$ | $V_{eff}$ (Gpc$^3$) | $V$ (Gpc$^3$) |
|---|---|---|---|---|
| $0.2 < z < 0.5$ | NGC | 429 182 | 2.7 | 4.7 |
| | SGC | 174 819 | 1.0 | 1.7 |
| | Total | 604 001 | 3.7 | 6.4 |
| $0.4 < z < 0.6$ | NGC | 500 872 | 3.1 | 5.3 |
| | SGC | 185498 | 1.1 | 2.0 |
| | Total | 686 370 | 4.2 | 7.3 |
| $0.5 < z < 0.75$ | NGC | 435 741 | 3.0 | 9.0 |
| | SGC | 158 262 | 1.1 | 3.3 |
| | Total | 594 003 | 4.1 | 12.3 |

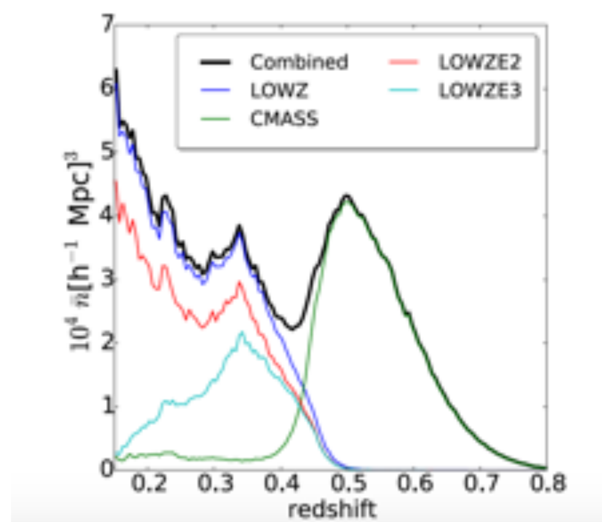

# Galaxy clustering: the signal

Analysis performed in configuration and Fourier space and gives consistent results

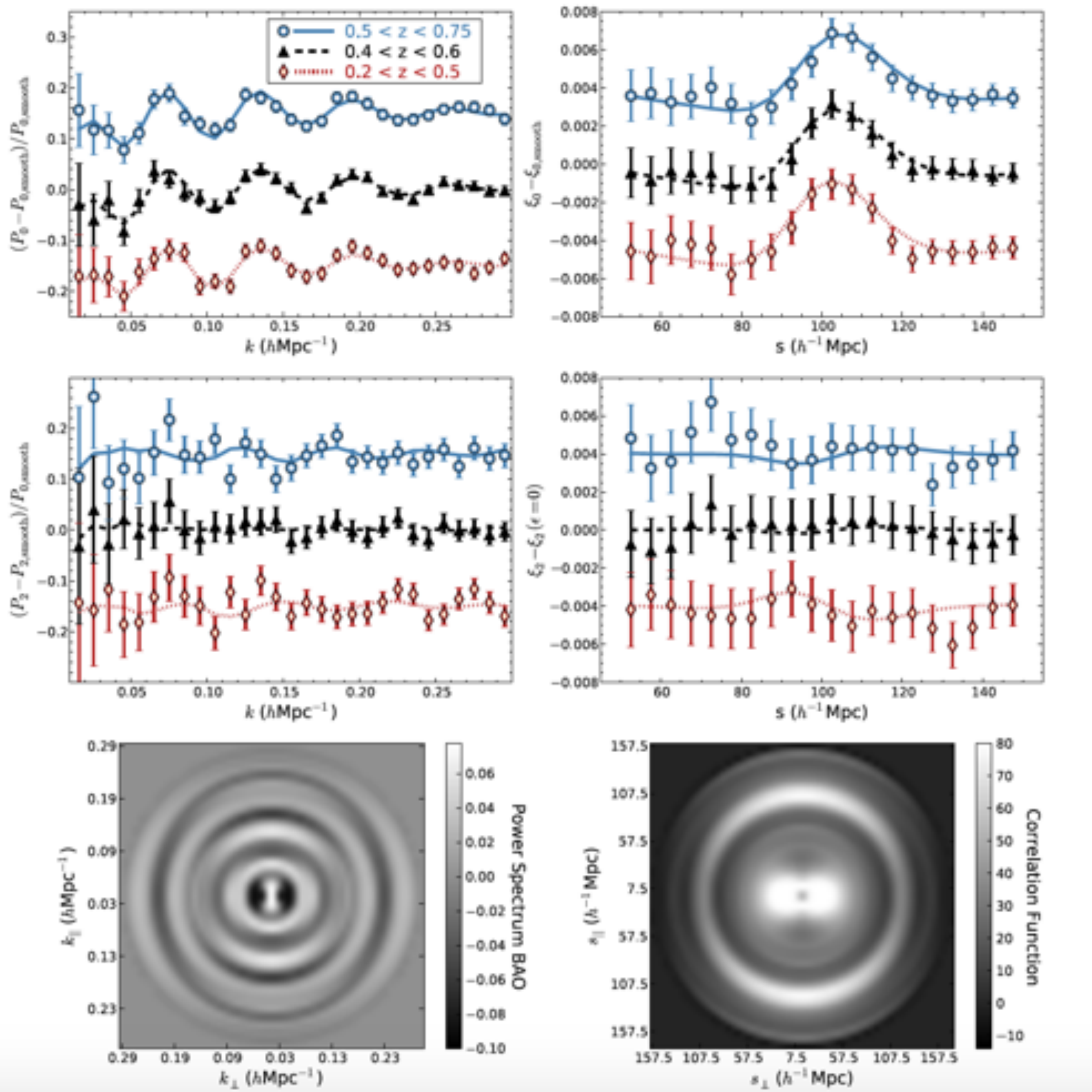

# Galaxy clustering: constraints from BAOs

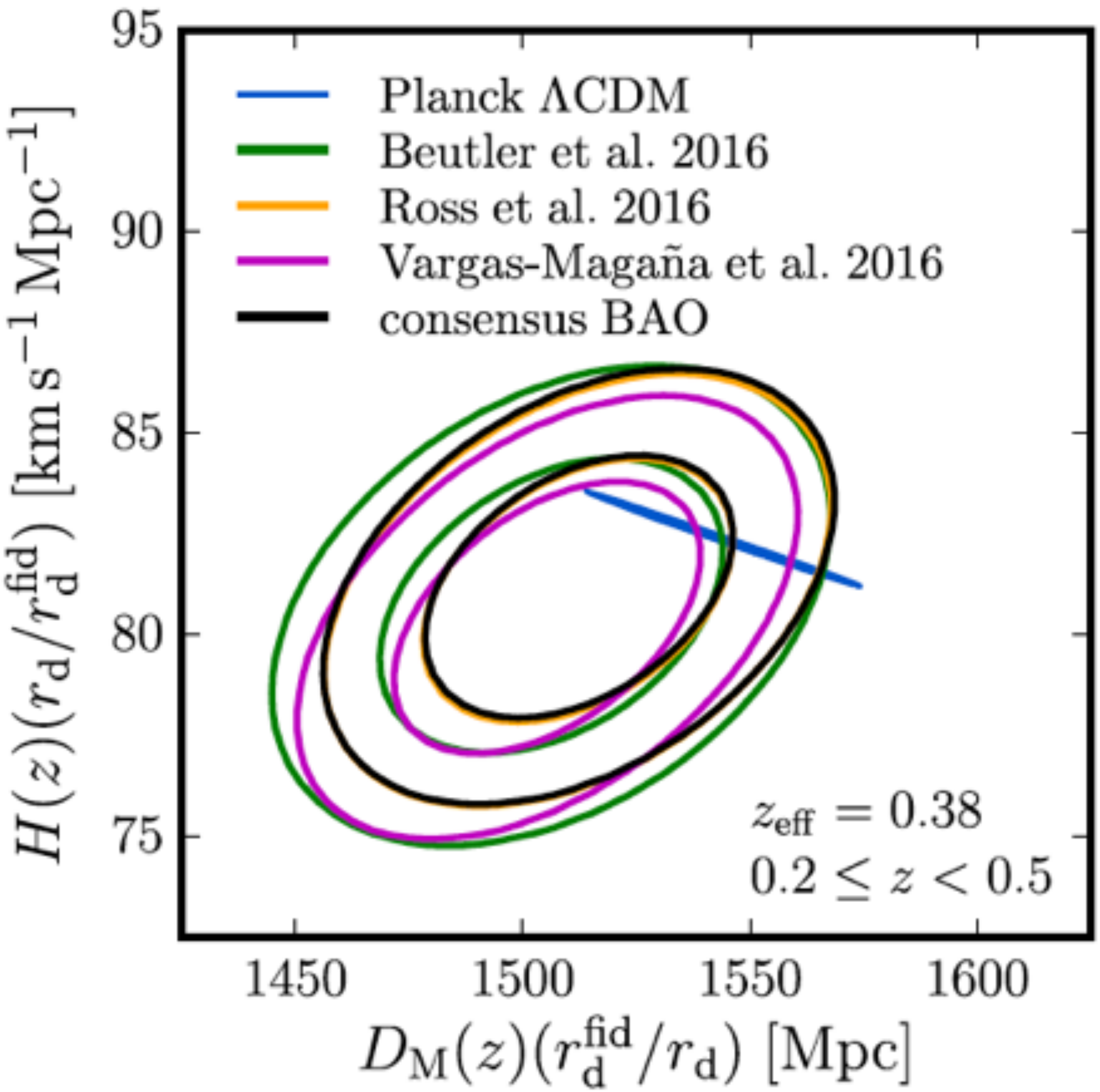


BAO measurement combined with CMB prior allows to measure H(z) at 2.4% and $D_A(z)$ at 1.5% in each redshift bin When combined $D_A(z)$ measured at 1% and H(z) at 1.6%

Perfect agreement with Planck

remarkable measurements not su much freedom to escape from LCDM

Consensus costraints are obtained by combined up to 7 different methods with strong covariance (mock estimated) but they improve the overall constraint significantly.

# Galaxy clustering: constraints from full shape

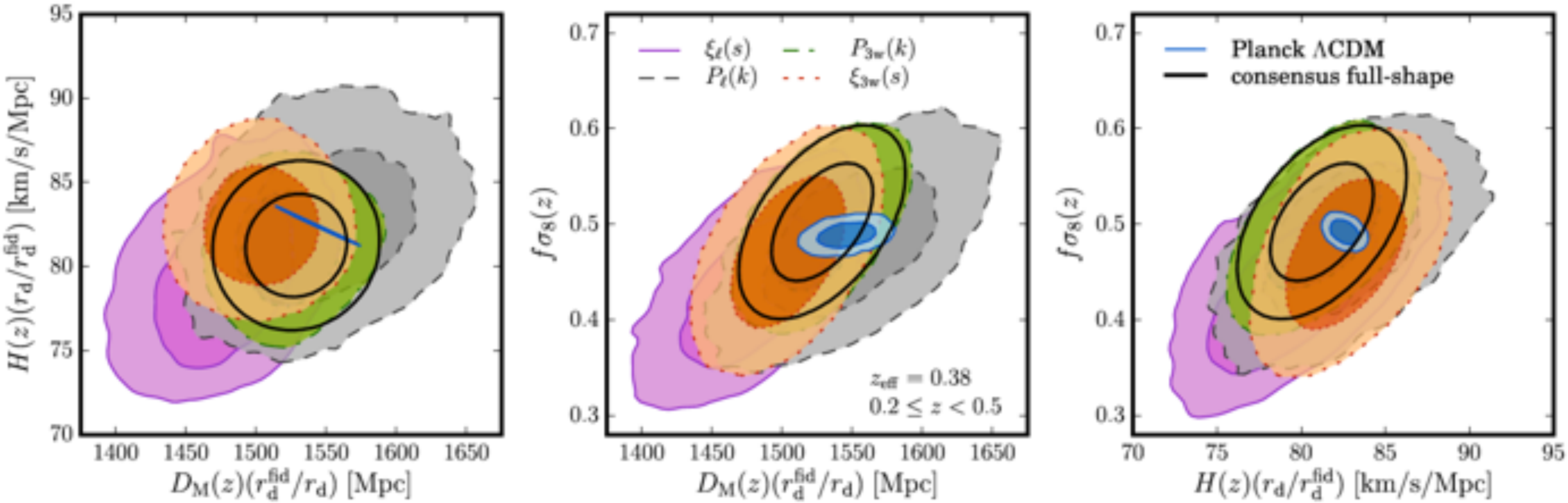


Full-shape measurement with a variety of methods, this allows to measure the $f\sigma_8$ combination with a 10% precision in each bin and overall a 6% measurement

Perfect agreement with Planck

# BAO+full shape combined

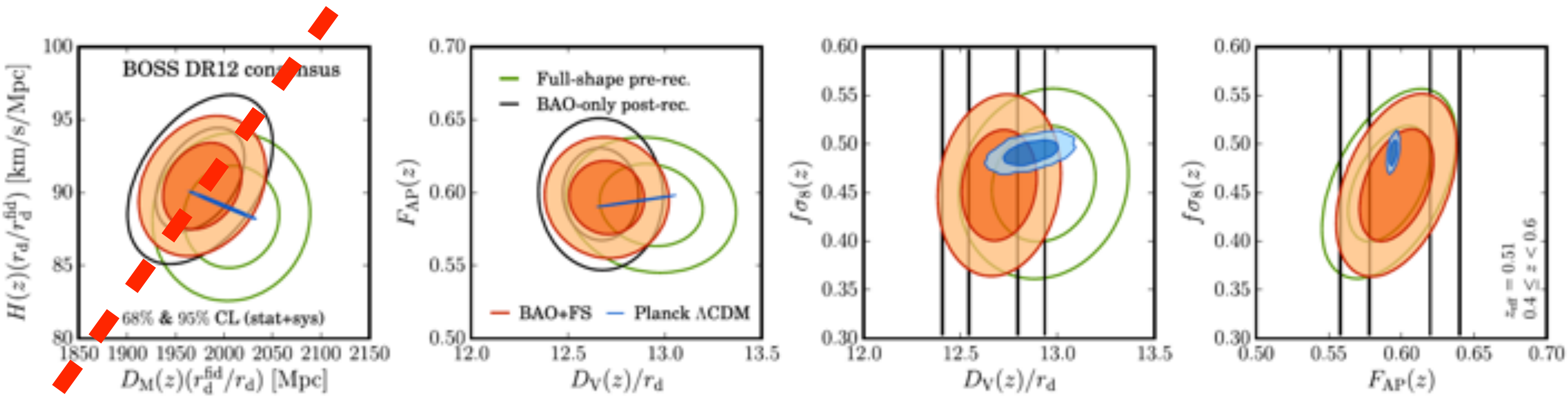


$D_M(z)$ and $H(z)$ are more strongly correlated for the BAO-only analysis, so while the $D_V(z)$ constraints from postreconstruction BAO-only are appreciably tighter than those from pre-reconstruction FS, the marginalized constraints on DM(z) and H(z) are not.

The constraints on $F_{AP}(z)$ from sub-BAO scales in the FS analyses help to **break the degeneracy** between $D_M$ and H, leading to rounder confidence contours and smaller errors on FAP.

Combined BAO+FS contours take advantage of both the **sharpening** of the BAO feature by reconstruction and the improved **degeneracy breaking from the sub-BAO Alcock–Paczynski effect.**

# Constraints from post-reconstruction BAO measurements and pre-reconstruction full-shape

statistical error

systematic error

| Measurement | Redshift | BAO only | Full shape | BAO + FS |
|---|---|---|---|---|
| $D_M(r_{\rm d,\,fid}/r_{\rm d})$ (Mpc) | $z = 0.38$ | $1512 \pm 22 \pm 11$ | $1529 \pm 24 \pm 11$ | $1518 \pm 20 \pm 11$ |
| $D_M(r_{\rm d,\,fid}/r_{\rm d})$ (Mpc) | $z = 0.51$ | $1975 \pm 27 \pm 14$ | $2007 \pm 29 \pm 15$ | $1977 \pm 23 \pm 14$ |
| $D_M(r_{\rm d,\,fid}/r_{\rm d})$ (Mpc) | $z = 0.61$ | $2307 \pm 33 \pm 17$ | $2274 \pm 36 \pm 17$ | $2283 \pm 28 \pm 16$ |
| $H(r_{\rm d}/r_{\rm d,\,fid})$ $(\rm km\,s^{-1}Mpc^{-1})$ | $z = 0.38$ | $81.2 \pm 2.2 \pm 1.0$ | $81.2 \pm 2.0 \pm 1.0$ | $81.5 \pm 1.7 \pm 0.9$ |
| $H(r_{\rm d}/r_{\rm d,\,fid})$ $(\rm km\,s^{-1}Mpc^{-1})$ | $z = 0.51$ | $90.9 \pm 2.1 \pm 1.1$ | $88.3 \pm 2.1 \pm 1.0$ | $90.5 \pm 1.7 \pm 1.0$ |
| $H(r_{\rm d}/r_{\rm d,\,fid})$ $(\rm km\,s^{-1}Mpc^{-1})$ | $z = 0.61$ | $99.0 \pm 2.2 \pm 1.2$ | $95.6 \pm 2.4 \pm 1.1$ | $97.3 \pm 1.8 \pm 1.1$ |
| $f\sigma_8$ | $z = 0.38$ | – | $0.502 \pm 0.041 \pm 0.024$ | $0.497 \pm 0.039 \pm 0.024$ |
| $f\sigma_8$ | $z = 0.51$ | – | $0.459 \pm 0.037 \pm 0.015$ | $0.458 \pm 0.035 \pm 0.015$ |
| $f\sigma_8$ | $z = 0.61$ | – | $0.419 \pm 0.036 \pm 0.009$ | $0.436 \pm 0.034 \pm 0.009$ |

# BAO Hubble Diagram

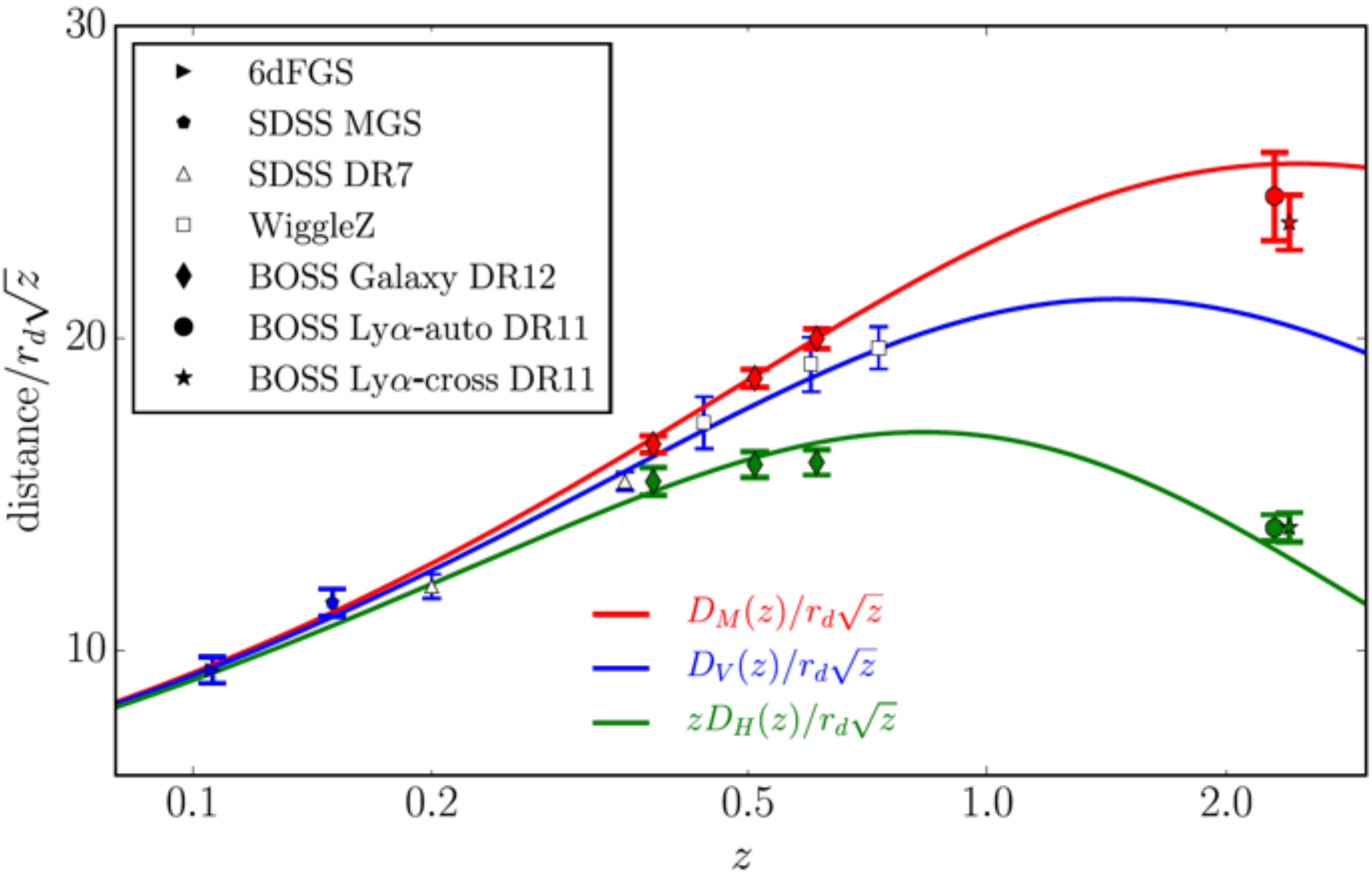

# RSD measurements from BOSS

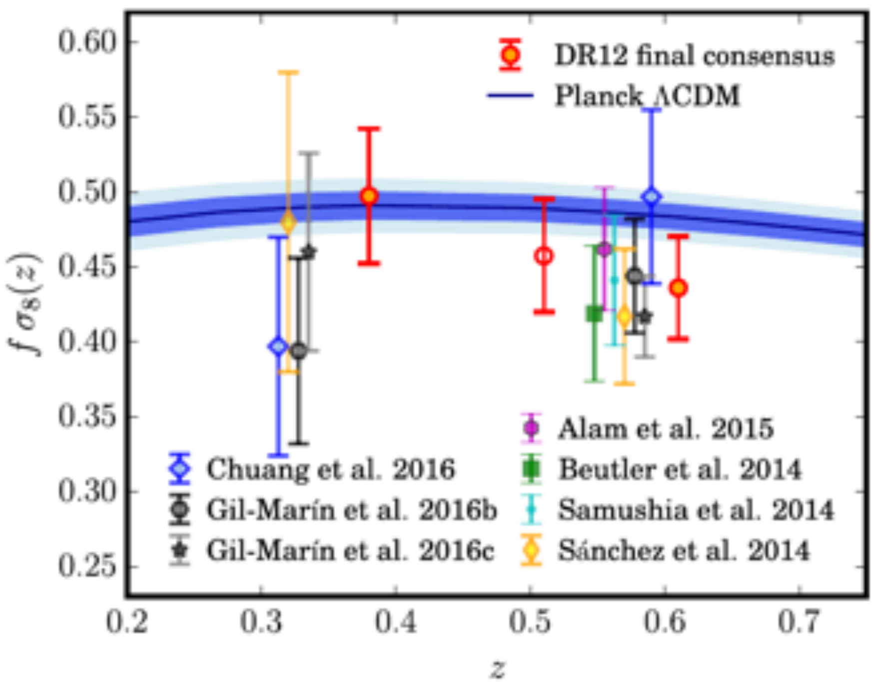


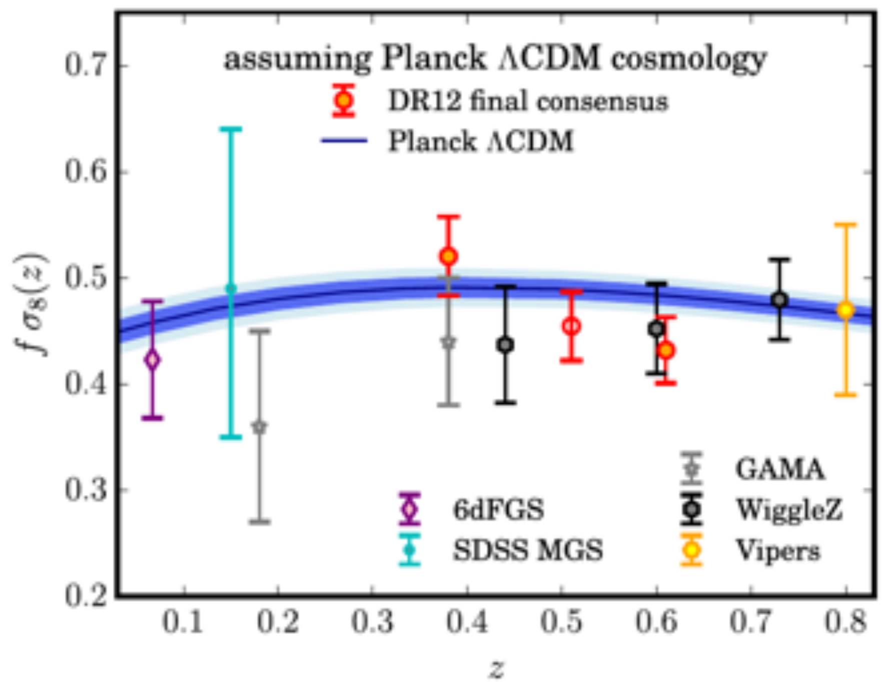

# Planck + BOSS galaxy clustering - I

In the LCDM case $\Omega_m$=0.311 ± 0.006 and $H_0$=67.6 ± 0.5 km/s/Mpc
If $\Omega_k$ and w are varied $\Omega_k$=0.0003 ± 0.0026 and w=-1.01 ± 0.06

owCDM model

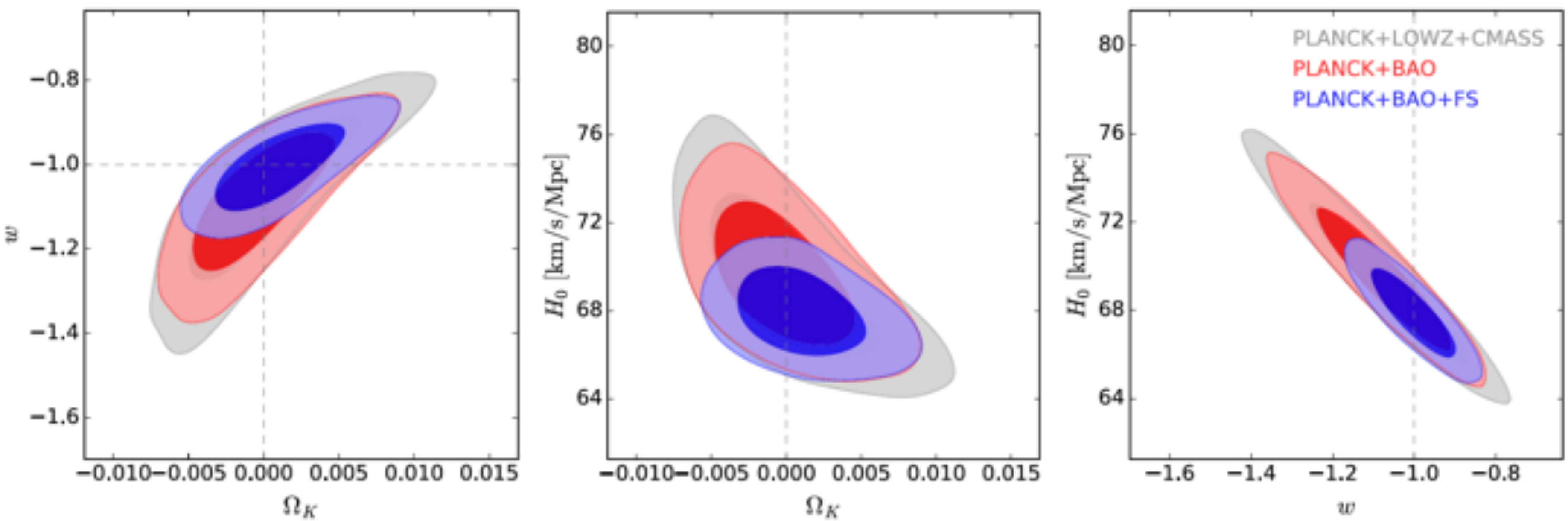


Main results:
1) impressive agreement with LCDM even after opening a 2 parameter space (w, $\Omega_k$)
2) FOM for wCDM ~20-30
3) Adding z-bins helps

# Planck + BOSS galaxy clustering - II

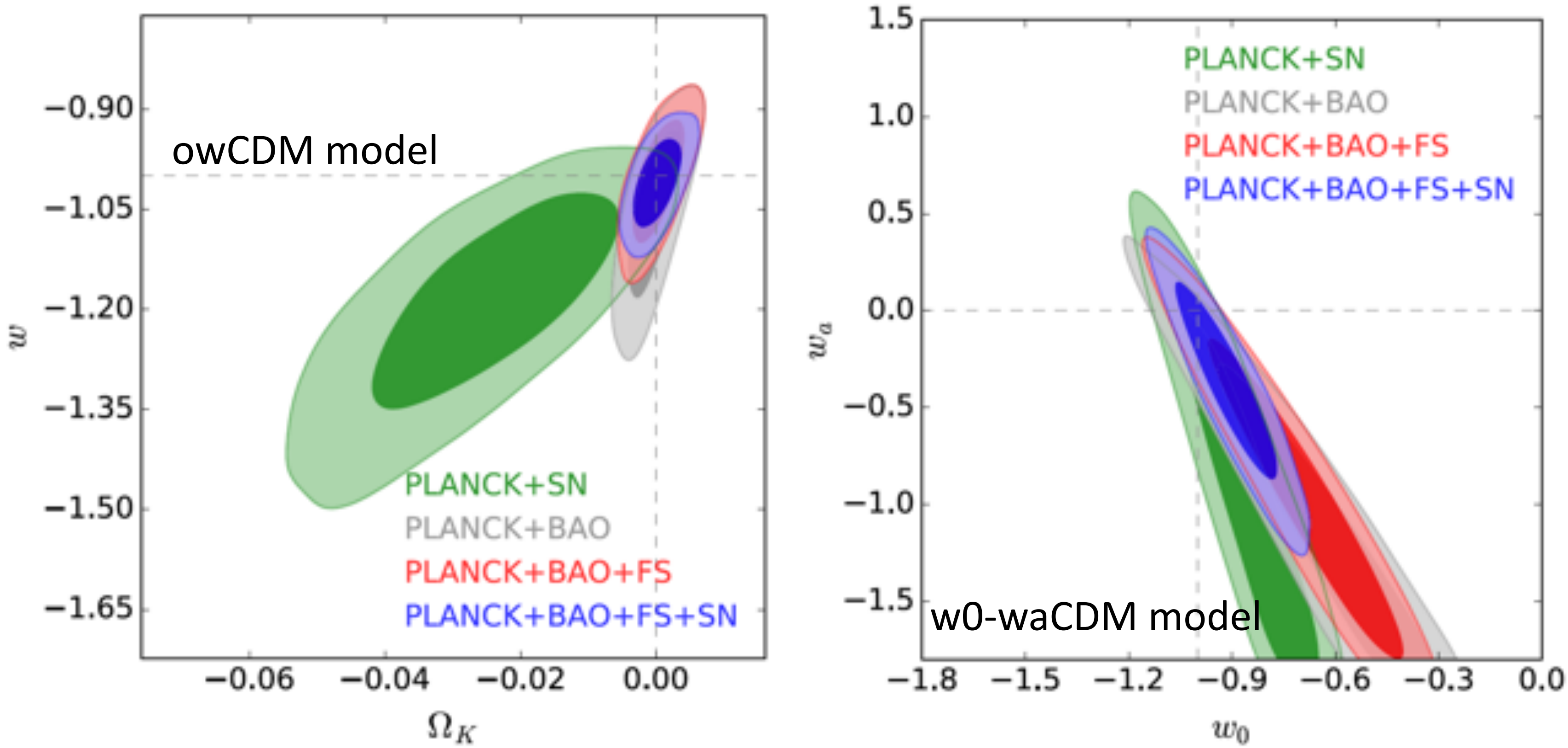


| Cosmological model | Data sets | $\Omega_m h^2$ | $\Omega_m$ | $H_0$ (km s$^{-1}$ Mpc$^{-1}$) | $\Omega_K$ | $w_0$ | $w_a$ |
|---|---|---|---|---|---|---|---|
| $w_0 w_a$CDM | Planck + SN | 0.1428 (14) | 0.294 (16) | 69.8 (18) | – | −0.85 (13) | −0.99 (63) |
| $w_0 w_a$CDM | Planck + BAO | 0.1427 (11) | 0.336 (21) | 65.2 (21) | – | −0.63 (20) | −1.16 (55) |
| $w_0 w_a$CDM | Planck + BAO + FS | 0.1427 (11) | 0.334 (18) | 65.5 (17) | – | −0.68 (18) | −0.98 (53) |
| $w_0 w_a$CDM | Planck + BAO + FS + SN | 0.1426 (11) | 0.313 (9) | 67.5 (10) | – | −0.91 (10) | −0.39 (34) |
| $ow_0 w_a$CDM | Planck + BAO | 0.1422 (14) | 0.331 (21) | 65.6 (21) | −0.0022 (30) | −0.66 (19) | −1.22 (53) |
| $ow_0 w_a$CDM | Planck + BAO + FS | 0.1422 (14) | 0.333 (16) | 65.4 (16) | −0.0020 (28) | −0.67 (18) | −1.12 (59) |
| $ow_0 w_a$CDM | Planck + BAO + FS + SN | 0.1420 (14) | 0.314 (10) | 67.3 (10) | −0.0023 (28) | −0.87 (11) | −0.63 (45) |

# Planck + BOSS galaxy clustering - III

$$f\sigma_8 \rightarrow f\sigma_8\left[A_{f\sigma_8} + B_{f\sigma_8}(z - z_{\rm p})\right]$$

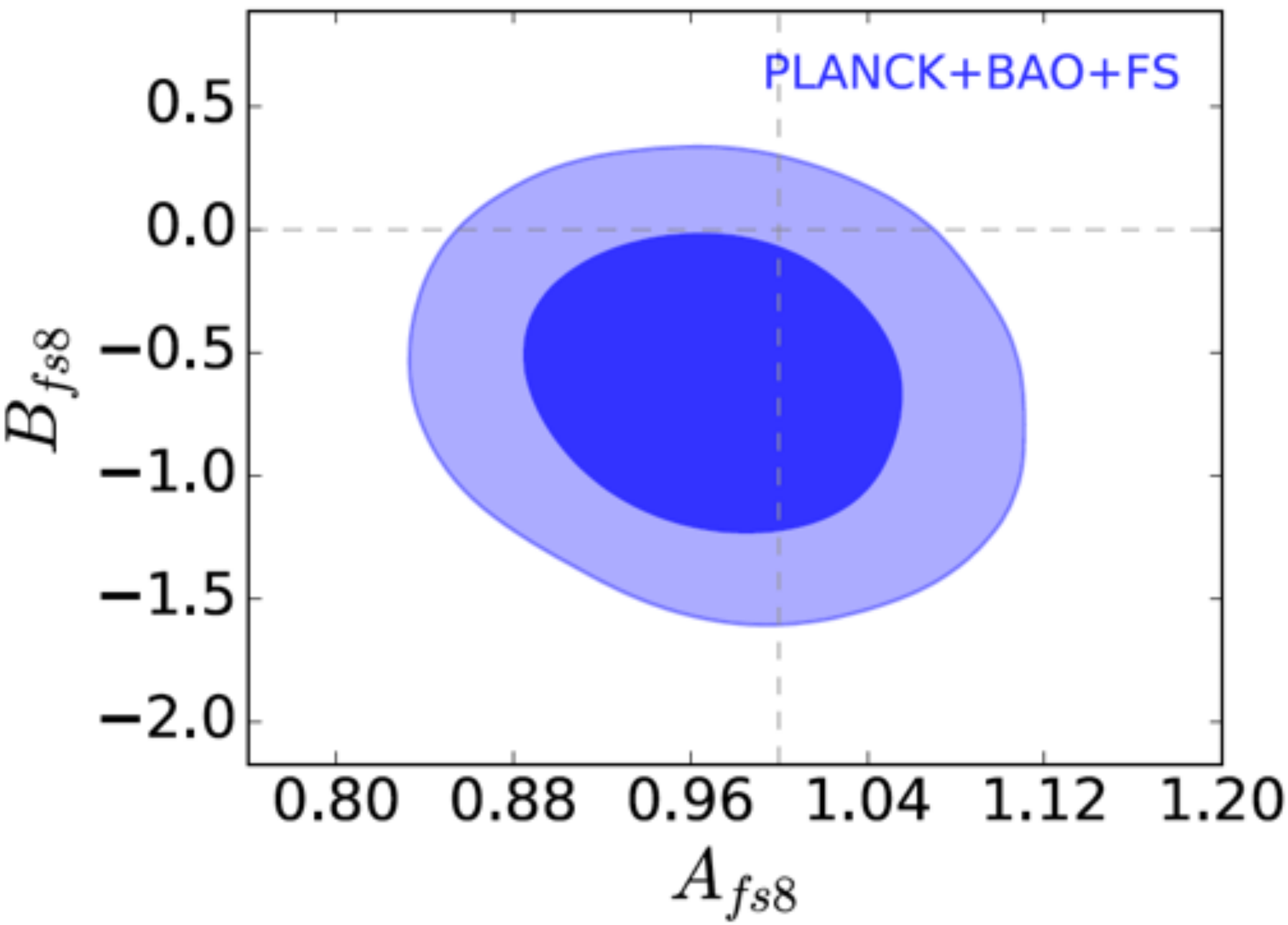


few percent offset from GR case - this is not significant

B is different from zero at 1.5sigma

6% error on A

Again very stable also when curvature and w are considered

# BOSS: main conclusions

1) ~1% constraints on H(z) and DA(z) from BAO

2) amplitude of pec. vel. measured at ~10% level

3) No evidence for physics beyond LCDM

4) Agreement with Planck low values for H0, with limits remarkably stable also for owCDM or ow0waCDM models with 1sigma error bar of 1km/s/Mpc

5) Limits on neutrino mass are 0.16 eV, which become 0.25 when removing RSD and ~0.3 when opening the w parameter space

6) No support for Neff>3

*OVERALL the stage is set and future seems promising for the next experimentslike eBO SS, DESI, WFIRST, Euclid etc.*
*it is expected that statistical errors will improve and a new level of systematics will be hit (sub-percent precision constraints)*

# DES 1yr results

Abbott+18

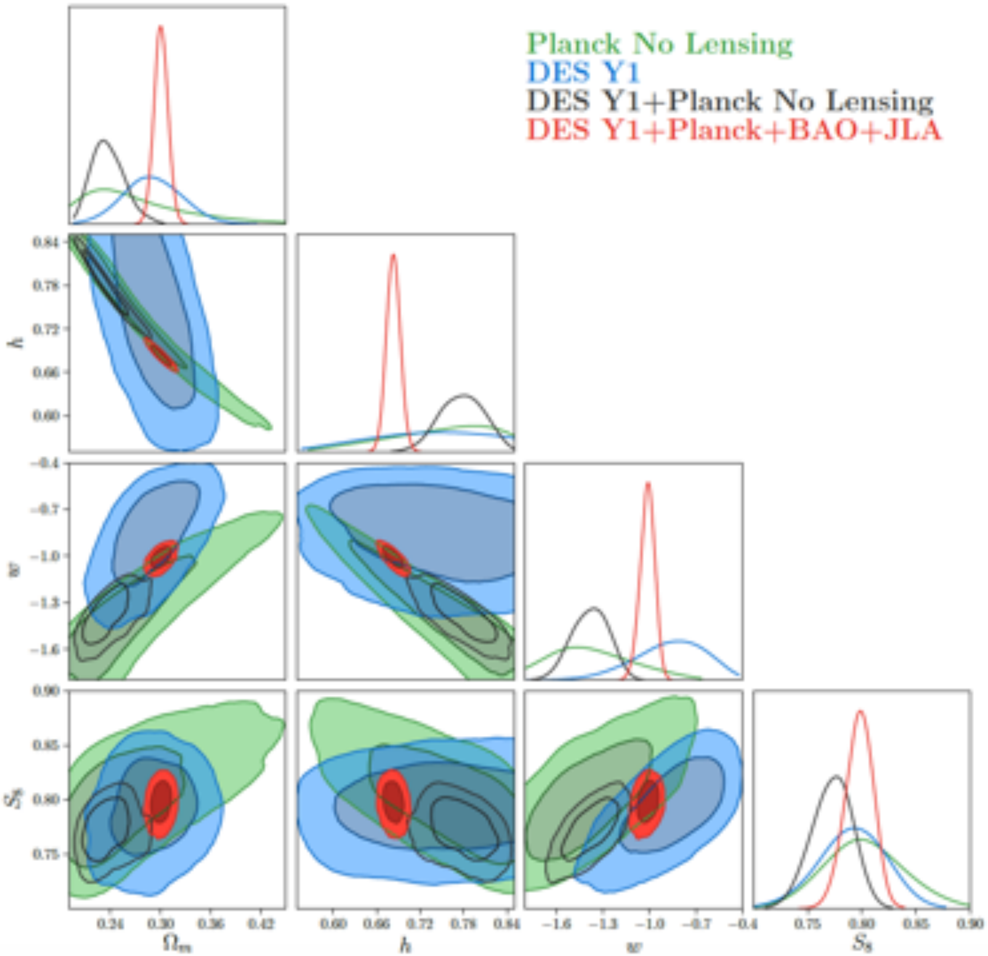


No preference for the addition of a free dark energy equation of state parameter.

Similar constraining power from WL and GC+GG lensing in terms of w.

The wCDM likelihoods from DES and Planck each constrain w poorly.

Allowing w as a free parameter makes the two data sets less consistent (in terms of the Bayesian evidence) and does not bring the DES and Planck central values of $S_8$ closer.

DES is, however, consistent with the bundle of Planck, BAO, and supernova data, and this combination constrains the equation-of-state parameter w = -1 ± 0.05.

| | | $w$ |
|---|---|---|
| $w$CDM | DES Y1 $\xi_{\pm}(\theta)$ | $-0.82^{+0.26}_{-0.47}$ |
| $w$CDM | DES Y1 $w(\theta)+\gamma_t$ | $-0.76^{+0.19}_{-0.45}$ |
| $w$CDM | DES Y1 3x2 | $-0.80^{+0.20}_{-0.22}$ |
| $w$CDM | Planck (No Lensing) | $-1.50^{+0.34}_{-0.18}$ |
| $w$CDM | DES Y1 + Planck (No Lensing) | $-1.34^{+0.08}_{-0.15}$ |
| $w$CDM | Planck + JLA + BAO | $-1.03^{+0.05}_{-0.05}$ |
| $w$CDM | DES Y1 + Planck + JLA + BAO | $-1.00^{+0.04}_{-0.05}$ |

# BAO constraints at high and low redshift

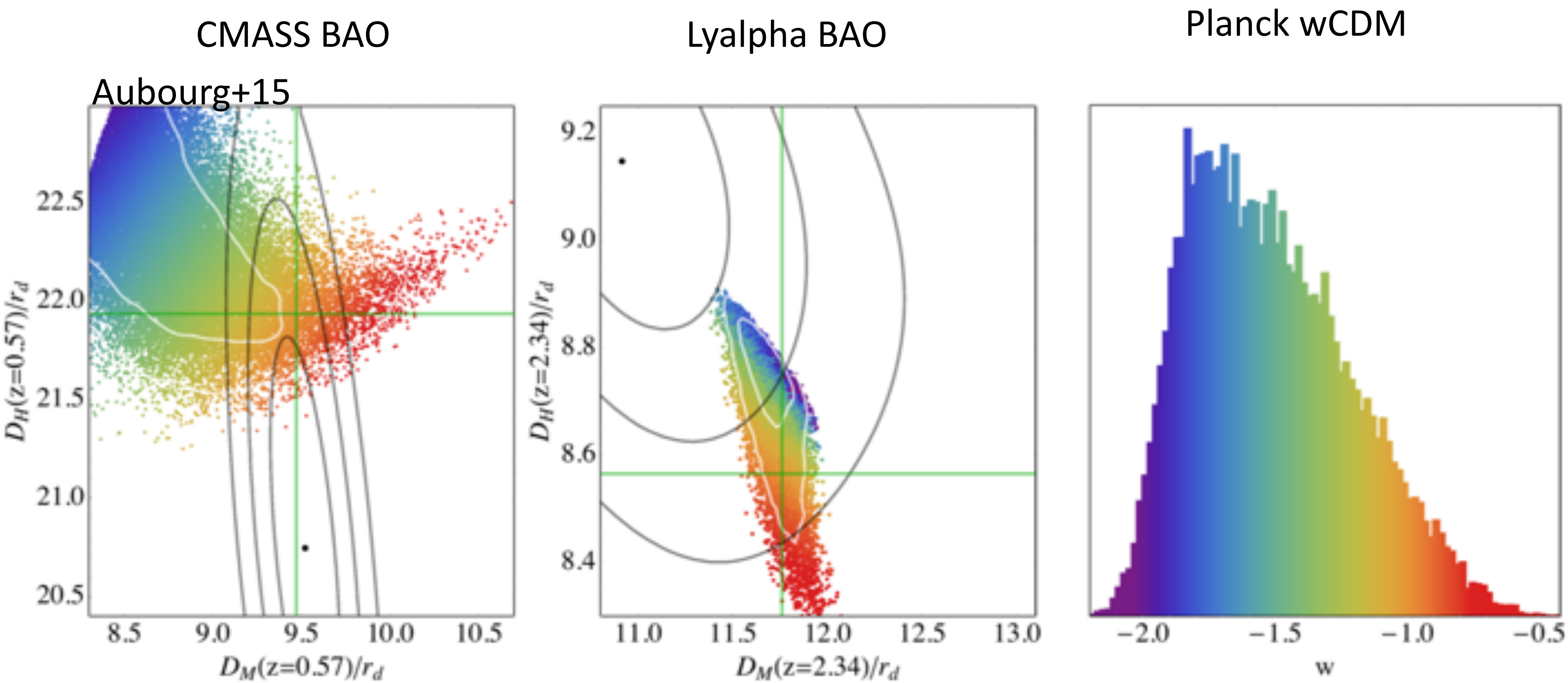


Tensions between Lya BAO and CMASS BAO

In general Early DE models can alleviate tensions of LCDM (low clustering amplitude and large $H_0$ are predicted at low z)

# Lyman-alpha BAO: a tuned oscillation?

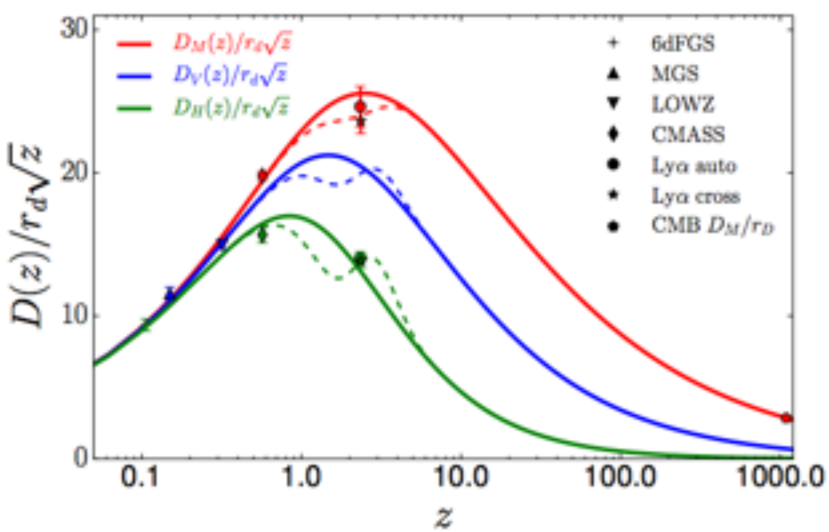


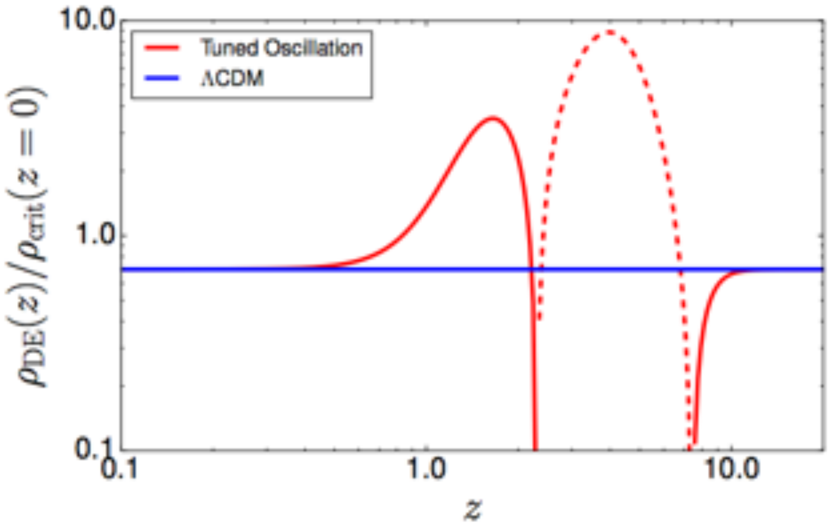


$\Delta\chi^2$=-6.6 with 3 d.o.f. for this model

# Future seems bright

DESI paper (2016) - stage IV experiment

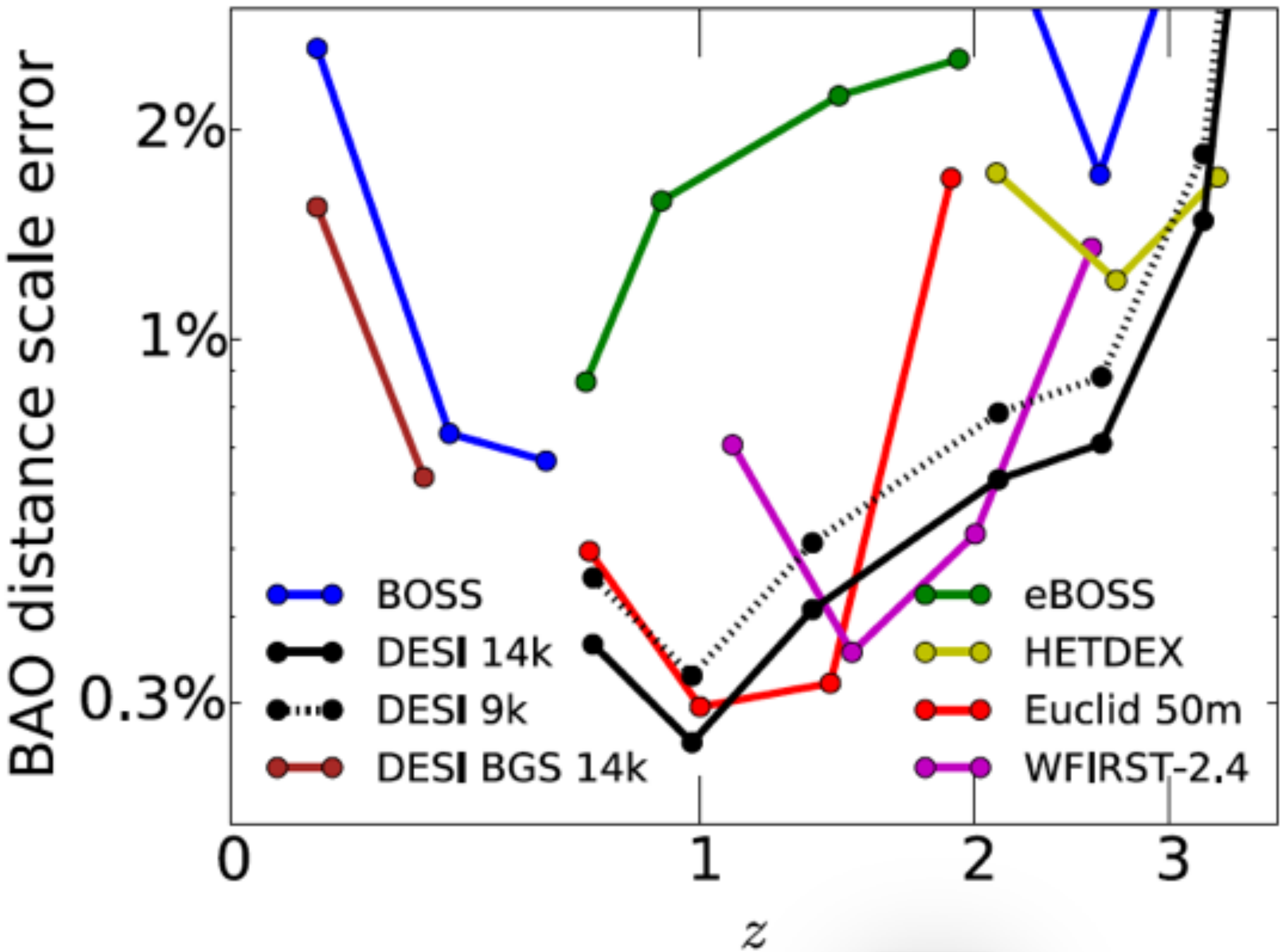

# Euclid

Euclid definition study report 2011

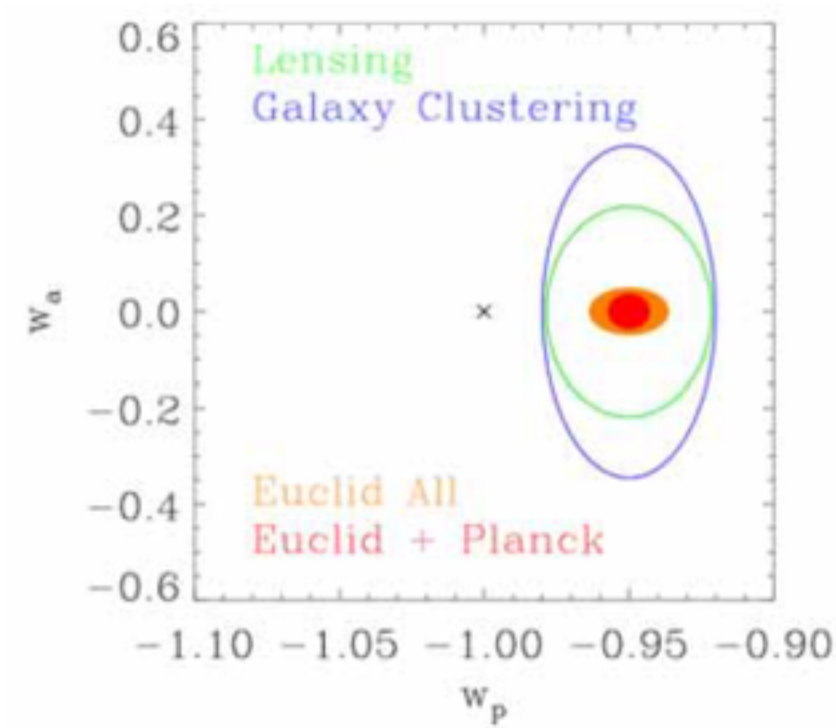


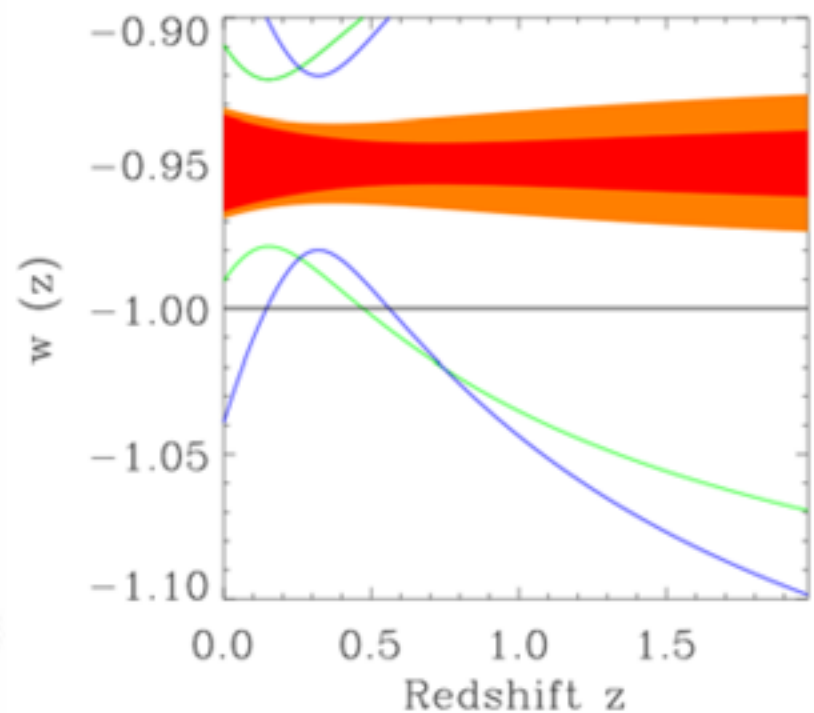


GC+WL

GC+WL+GCs+ISW

| | Dark Energy | | |
|---|---|---|---|
| **Parameter** | $w_p$ | $w_a$ | *FoM* |
| Euclid Primary | 0.015 | 0.150 | 430 |
| Euclid All | 0.013 | 0.048 | 1540 |
| Euclid+Planck | 0.007 | 0.035 | 4020 |
| Current | 0.100 | 1.500 | ~10 |
| **Improvement Factor** | **>10** | **>50** | **>300** |

# DESI constraints

**Table 2.9:** DETF Figures of Merit and uncertainties $\sigma_{w_p}$ and $\sigma_{\Omega_k}$. $\sigma_{w_p}$ is the error on $w$ at the pivot redshift, which also equal to the error on a constant $w$ holding $w_a = 0$. $\sigma_{\Omega_k}$ is the error on the curvature of the Universe, $\Omega_k$. All DESI lines contain the BGS, and BOSS in the range $0.45 < z < 0.6$ that does not substantially overlap with DESI. All cases include *Planck* CMB constraints. The pivot point, where $w(a)$ has minimal uncertainty is indicated by $a_p$. We note that a FoM of 110 is 10 times the Stage II level of [109], which we take to be the definition of Stage IV. DESI BAO galaxy exceeds this threshold even with a 9,000 square degree survey.

| Surveys | FoM | $a_p$ | $\sigma_{w_p}$ | $\sigma_{\Omega_k}$ |
|---|---|---|---|---|
| BOSS BAO | 37 | 0.65 | 0.055 | 0.0026 |
| DESI 14k galaxy BAO | 133 | 0.69 | 0.023 | 0.0013 |
| DESI 14k galaxy and Ly-$\alpha$ forest BAO | 169 | 0.71 | 0.022 | 0.0011 |
| DESI 14k BAO + gal. broadband to $k < 0.1\ h\ \mathrm{Mpc}^{-1}$ | 332 | 0.74 | 0.015 | 0.0009 |
| DESI 14k BAO + gal. broadband to $k < 0.2\ h\ \mathrm{Mpc}^{-1}$ | 704 | 0.73 | 0.011 | 0.0007 |
| DESI 9k galaxy BAO | 95 | 0.69 | 0.027 | 0.0015 |
| DESI 9k galaxy and Ly-$\alpha$ forest BAO | 121 | 0.71 | 0.026 | 0.0012 |
| DESI 9k BAO + gal. broadband to $k < 0.1\ h\ \mathrm{Mpc}^{-1}$ | 229 | 0.73 | 0.018 | 0.0011 |
| DESI 9k BAO + gal. broadband to $k < 0.2\ h\ \mathrm{Mpc}^{-1}$ | 502 | 0.73 | 0.013 | 0.0009 |

# The WFIRST-2.4 Dark Energy Roadmap

## Supernova Survey

wide, medium, & deep imaging
+
IFU spectroscopy

2700 type Ia supernovae
$z = 0.1–1.7$

standard candle distances
$z < 1$ to 0.20% and $z > 1$ to 0.34%

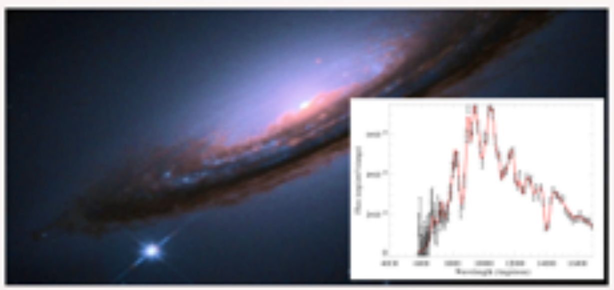

## High Latitude Survey

spectroscopic: galaxy redshifts

20 million Hα galaxies, $z = 1–2$
2 million [OIII] galaxies, $z = 2–3$

imaging: weak lensing shapes

500 million lensed galaxies
40,000 massive clusters

standard ruler

| distances | expansion rate |
|---|---|
| $z = 1–2$ to 0.4% | $z = 1–2$ to 0.72% |
| $z = 2–3$ to 1.3% | $z = 2–3$ to 1.8% |

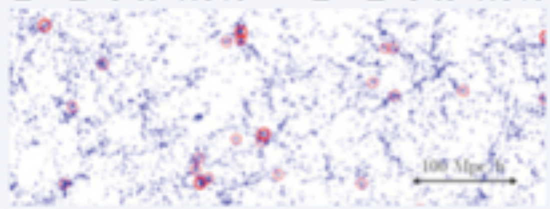

dark matter clustering
$z < 1$ to 0.16% (WL); 0.14% (CL)
$z > 1$ to 0.54% (WL); 0.28% (CL)
1.2% (RSD)

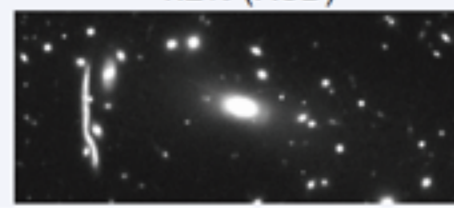

history of dark energy
+
deviations from GR

$w(z)$, $\Delta G(z)$, $\Phi_{REL}/\Phi_{NREL}$

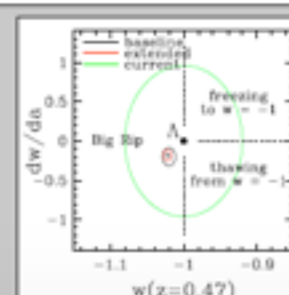

Cosmology with the WFIRST High Latitude Survey Science Investigation Team
Annual Report 2017 arXiv: 1804.03628

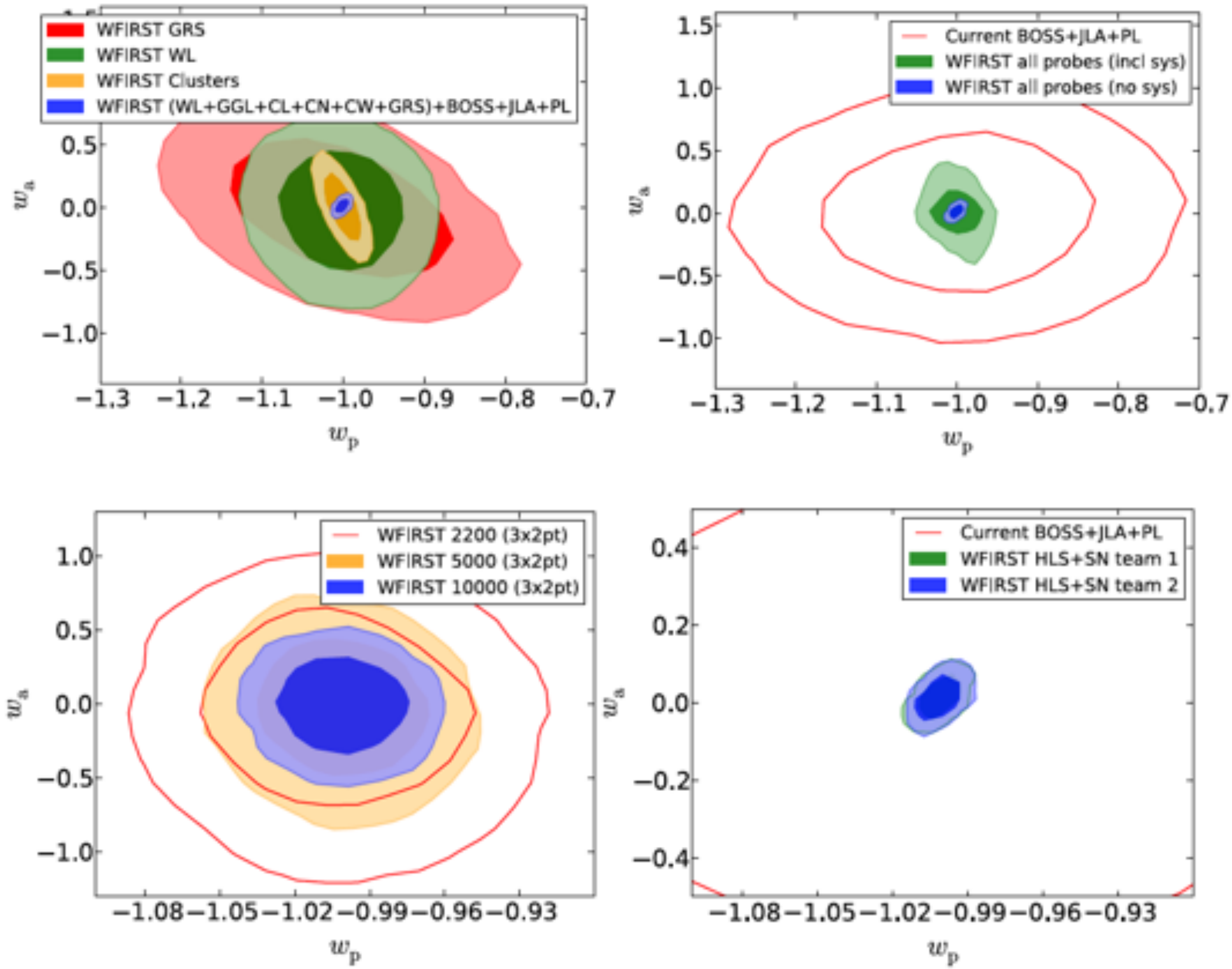

# Dark Energy Experiments: 2013 - 2031

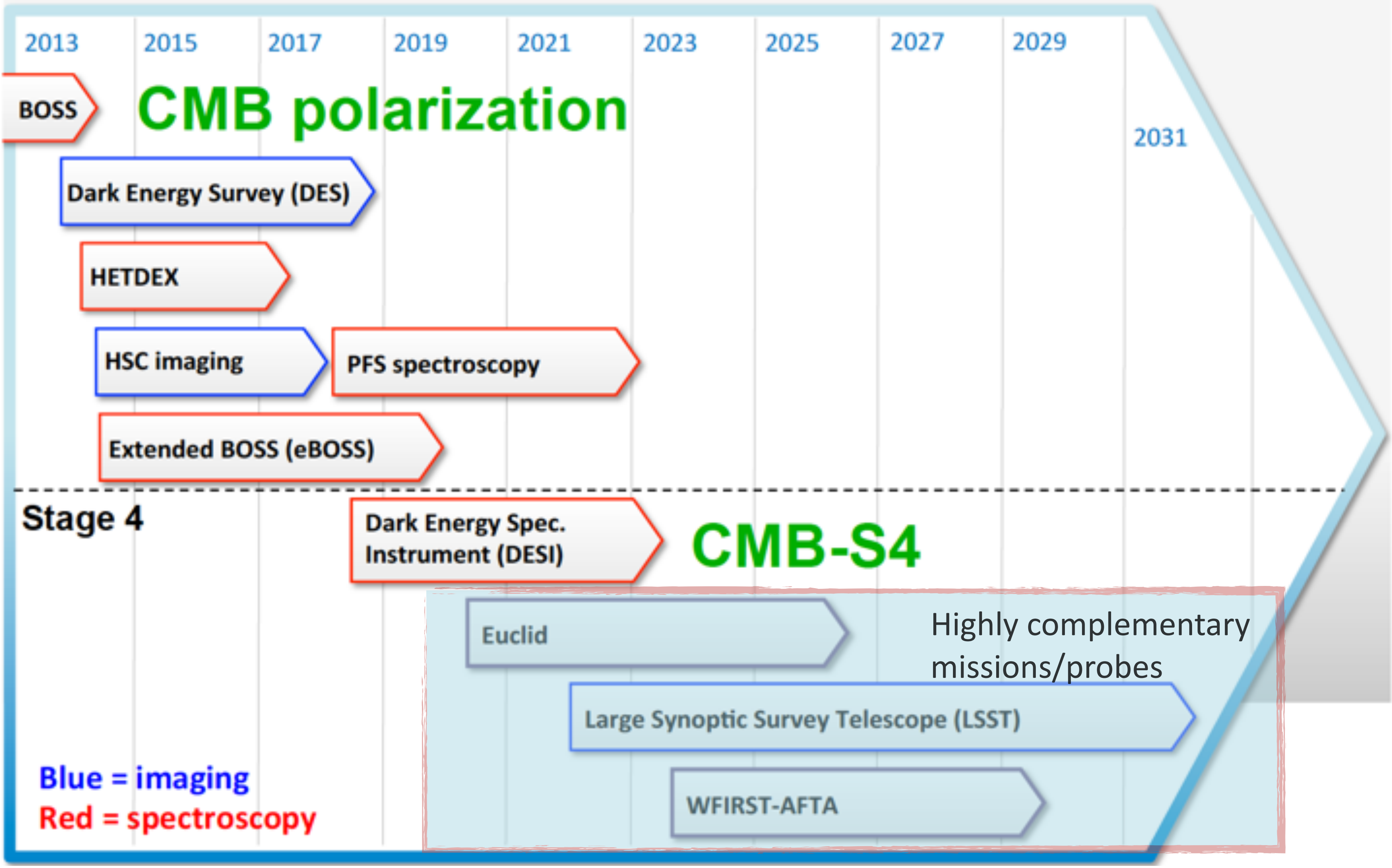

# Challenges of GC studies for dark energy

- bias modelling at mildly non-linear scales to exlpoit also other smaller volume surveys

- neutrino mass measurement and modelling of neutrino induced non-linearities in GCs (scale dependence of the bias)

- higher order statistics and the search for non-Gaussianities

- Cross correlations

- Multi purpose experiments with high degree of complementarity

- Machine learning and data science (pixel-by-pixel analysis)

- **High redshift regime/huge discovery potential**

*Cosmic Visions Dark Energy 2016*

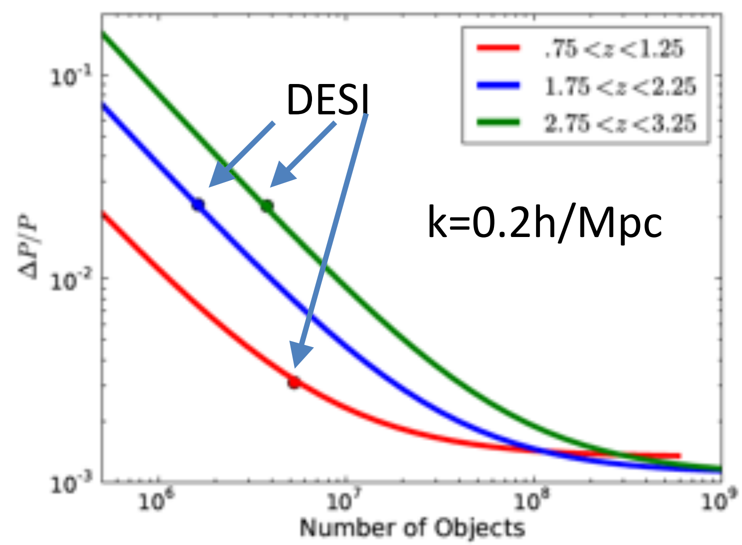


*Ultimate error achievable on the power spectrum (maximum amount of information in the sky)*

# SDSS/BOSS - II: detection of the BAO peak

Busca et al. 13

$$\xi_{\rm cosmo}(r_\parallel, r_\perp) = \xi_{\rm smooth}(r_\parallel, r_\perp) + a_{\rm peak} \cdot \xi_{\rm peak}(r_\parallel \alpha_\parallel, r_\perp \alpha_\perp)$$

$$\xi(r_\parallel, r_\perp) = \xi_{\rm cosmo}(r_\parallel, r_\perp, \alpha_\parallel, \alpha_\perp) + \xi_{\rm bb}(r_\parallel, r_\perp)$$

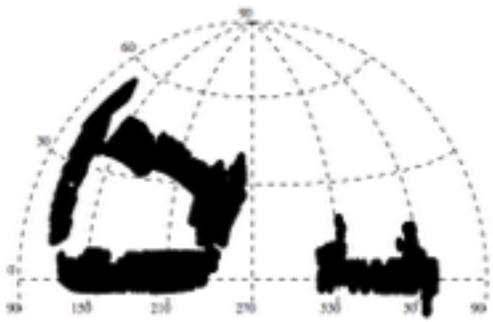

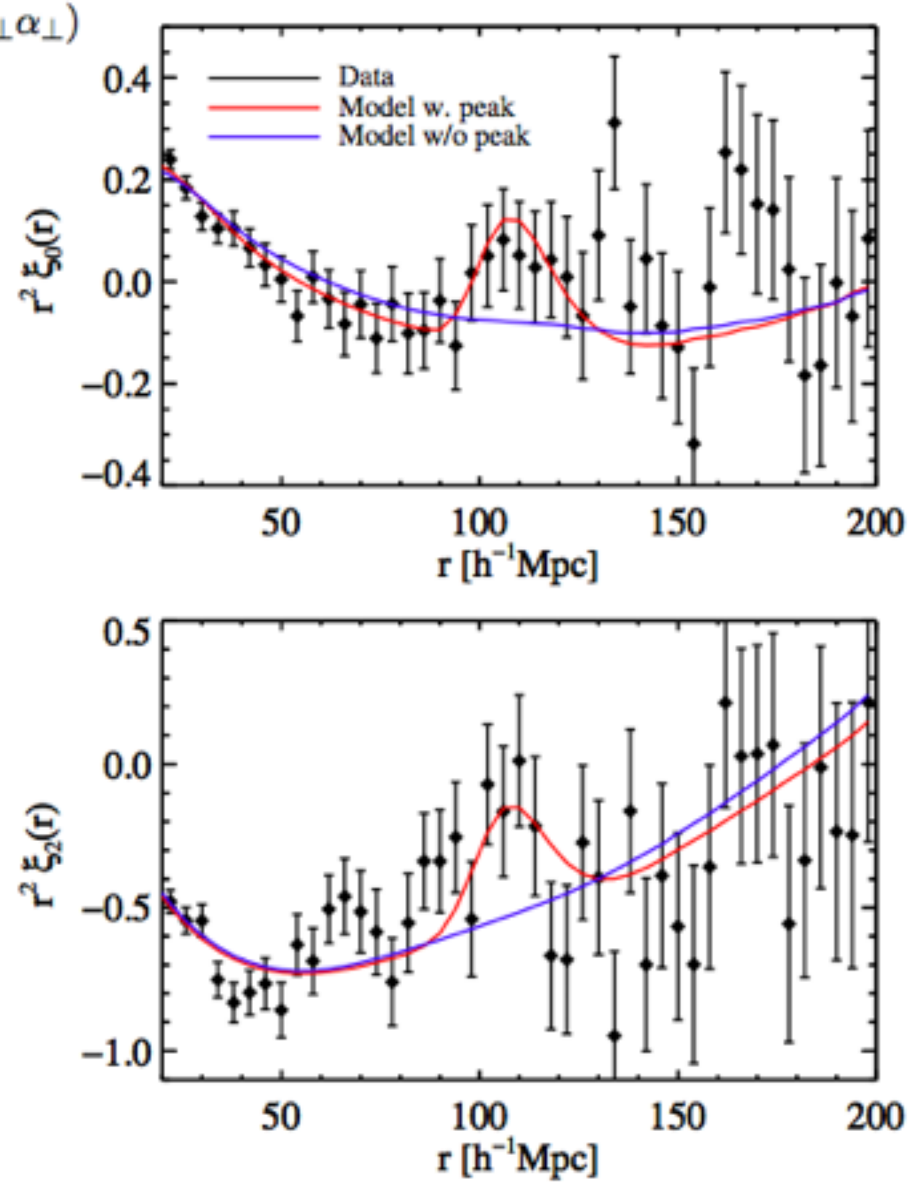


BAO feature detected at z=2.3
From 3000 deg$^2$, using 50000 QSOs
Significance of the detection at around 3$\sigma$

## SDSS/BOSS-III: cross-correlation with QSOs

$$P_{qF}(\mathbf{k}) = b_q \left[1 + \beta_q \mu_k^2\right] b_F \left[1 + \beta_F \mu_k^2\right] \, P(k)$$

6% precision measurement of $D_A/r_d$

3% precision measurement of $D_H/r_d$

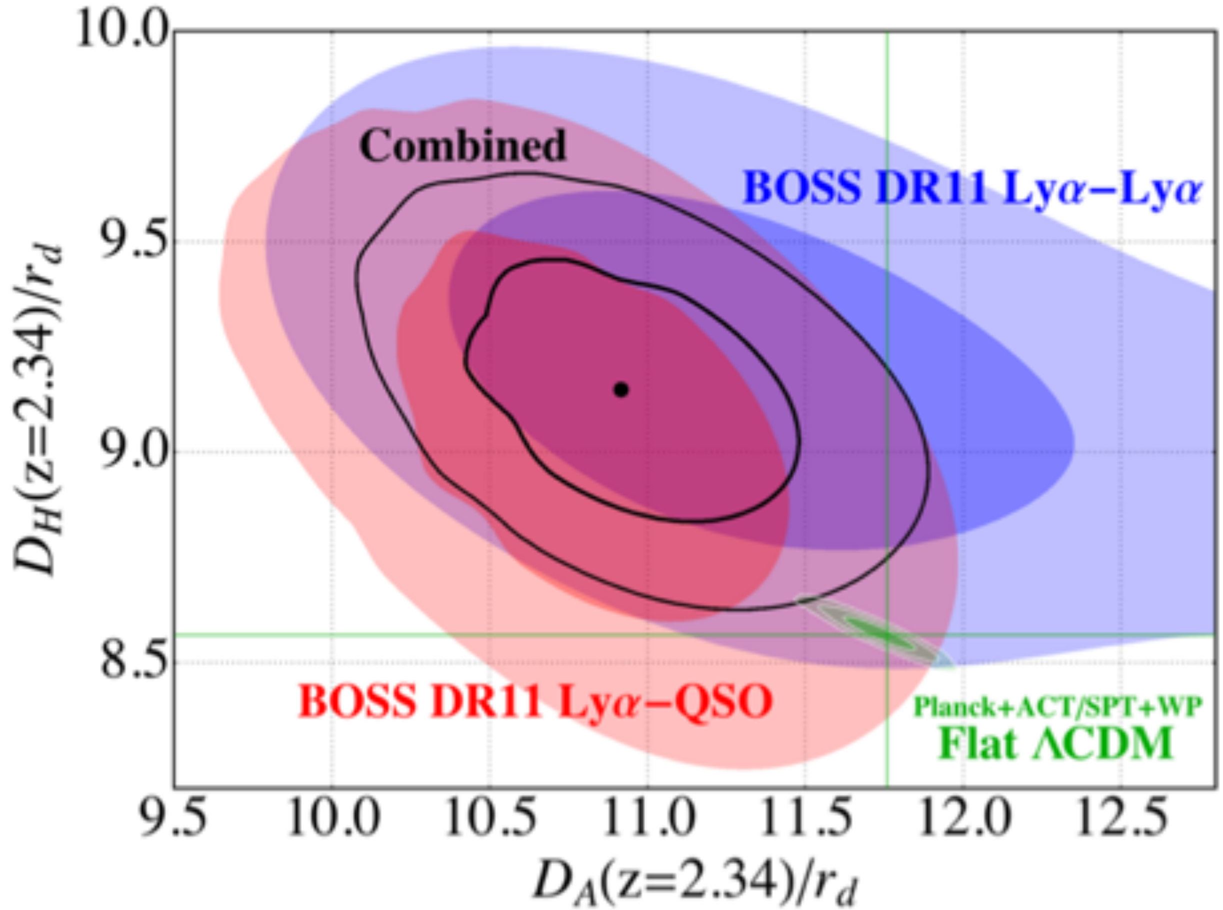


Delubac et al. 14

## SDSS/BOSS-IV: final data release

Bautista+ 17, arXiv: 1702.00176

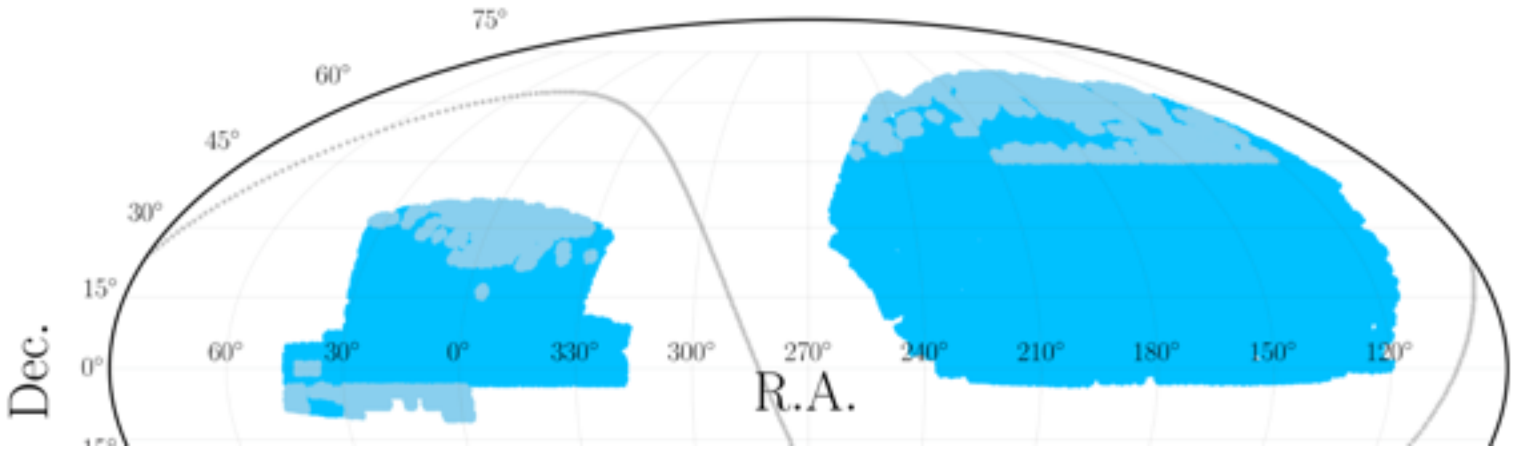


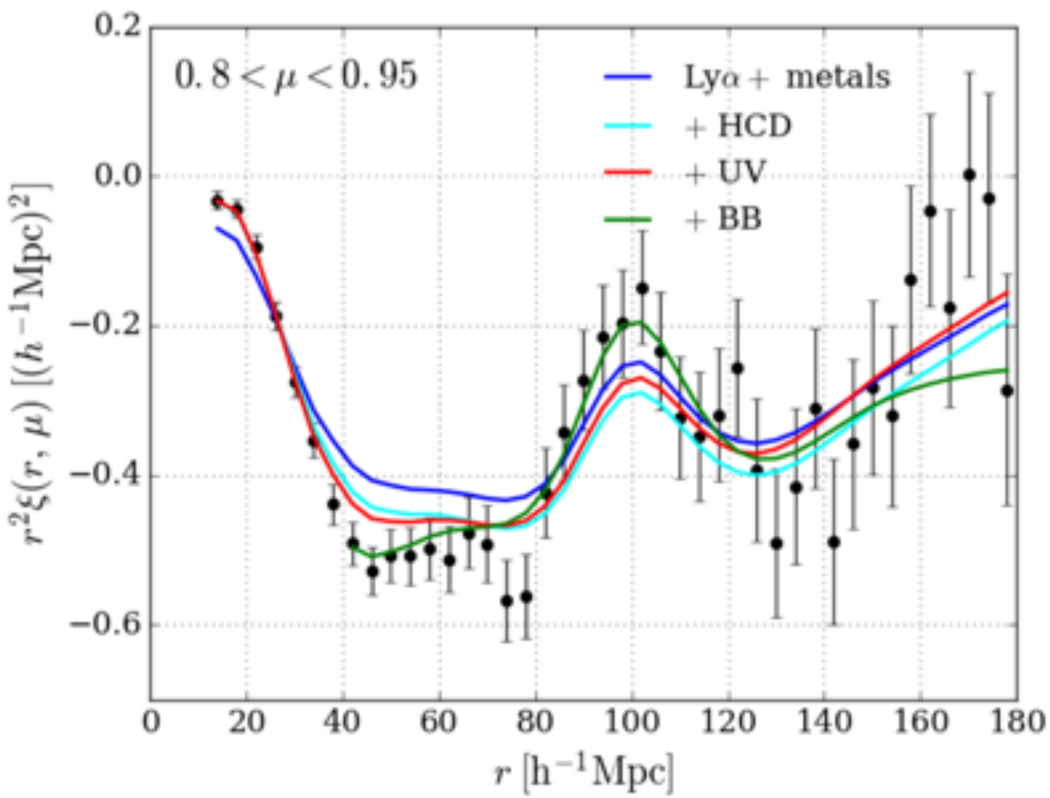


Flux correlation function in mu bin (nearly parallel to line-of-sight)

## SDSS/BOSS-IV: cosmological implications

Bautista+ 17, arXiv: 1702.00176

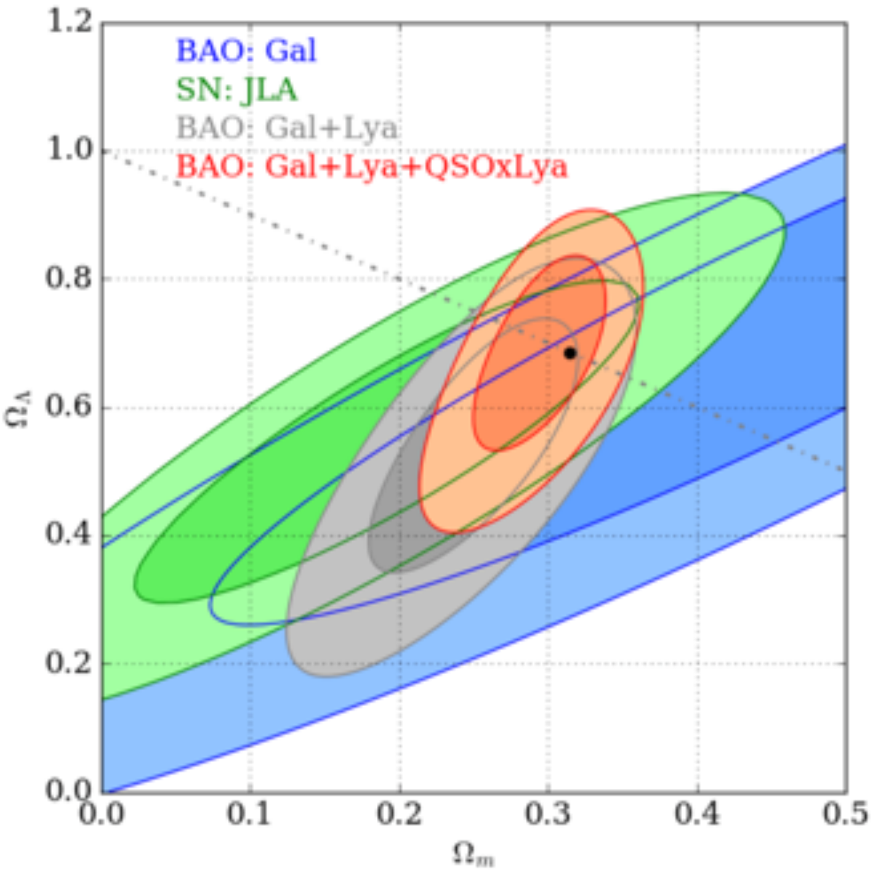


- Redshift covered z=2.1-3.5, <z>=2.33.
- 160,000 QSOs (DESI will have ~ 10 times more.
- Statistical improvement over DR9, DR11 (Delubac+14) hinted for a change in the sign of dark energy density to reconcile with Planck.
- Better physical modelling for high column density systems, UV fluctuations, broad band power (marginalized over).
- Complementarity with low redshift BAO, high redshift BAO provide a stronger support for $\Omega_\Lambda > 0$ (independent of CMB).

$$\Omega_M = 0.296 \pm 0.029 \qquad \Omega_\Lambda = 0.699 \pm 0.100$$

$$\Omega_k = -0.002 \pm 0.119$$

# SKA

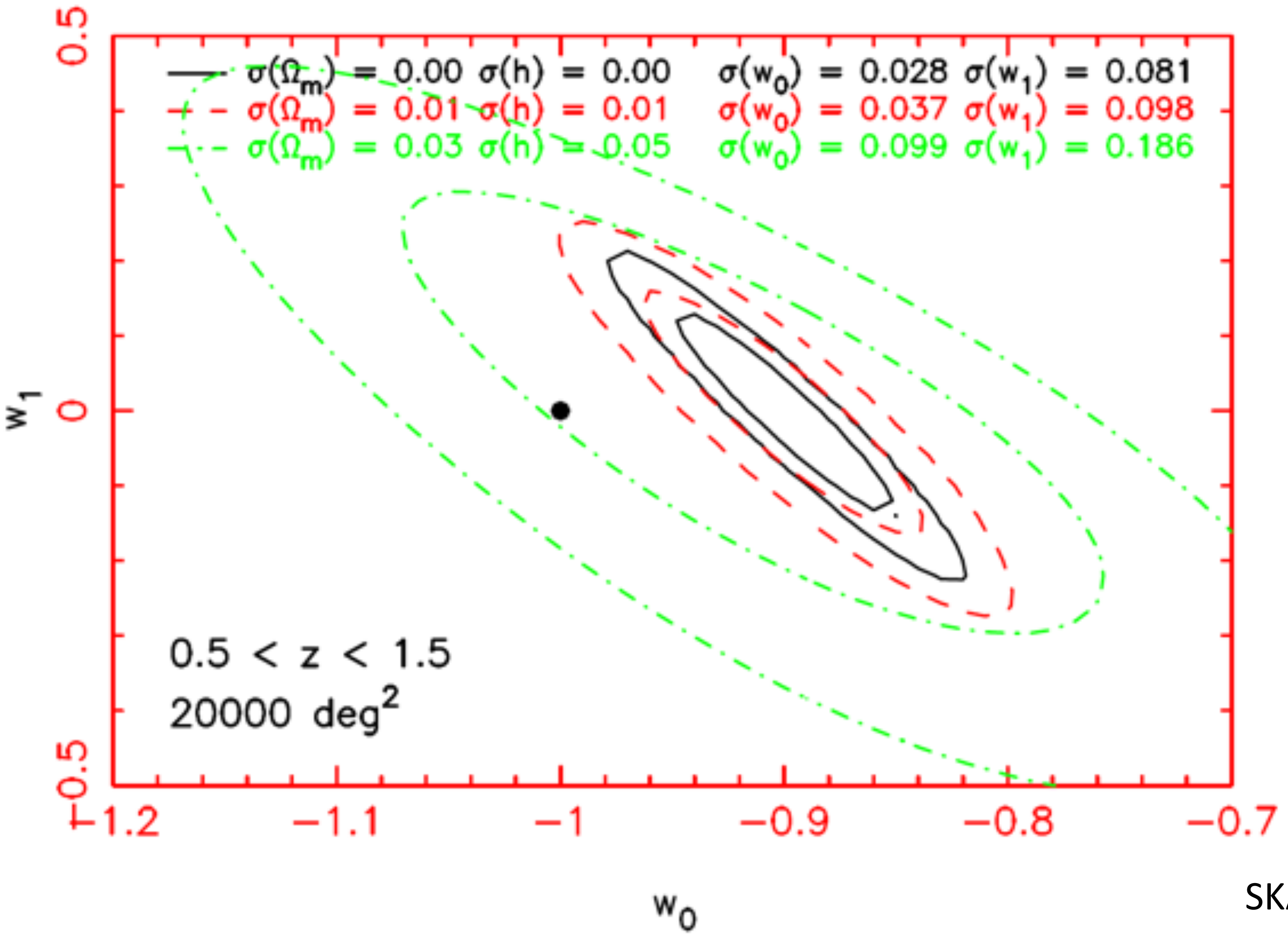


SKA Whitepaper 2005